AD 723961

AD

REPORT NO. RR-TR-71-2

THERMAL LASER EXCITATION BY SUPERSONIC MIXING IN A GAS DYNAMIC NOZZLE

by

H. Lee Davis

1 April 1971

DISTRIBUTION OF THIS DOCUMENT HAS BEEN APPROVED FOR PUBLIC RELEASE AND SALE; ITS DISTRIBUTION IS UNLIMITED.

U.S. ARMY MISSILE COMMAND
Redstone Arsenal, Alabama 35809

BEST AVAILABLE COPY

D D C
RECEIVED
JUN 1 1971
B

Reproduced by
NATIONAL TECHNICAL INFORMATION SERVICE
Springfield, Va. 22151

UNCLASSIFIED
Security Classification

DOCUMENT CONTROL DATA - R & D

(Security classification of title, body of abstract and indexing annotation must be entered when the overall report is classified)

1. ORIGINATING ACTIVITY *(Corporate author)* Physical Sciences Directorate Directorate for Res, Dev, Eng, & Msl Sys Lab US Army Missile Command Redstone Arsenal, Alabama 35809	2a. REPORT SECURITY CLASSIFICATION UNCLASSIFIED 2b. GROUP NA

3. REPORT TITLE

THERMAL LASER EXCITATION BY SUPERSONIC MIXING IN A GAS DYNAMIC NOZZLE

4. DESCRIPTIVE NOTES *(Type of report and inclusive dates)*

Technical Report

5. AUTHOR(S) *(First name, middle initial, last name)*

H. Lee Pratt

6. REPORT DATE	7a. TOTAL NO. OF PAGES	7b. NO. OF REFS
1 April 1971	88	39

8a. CONTRACT OR GRANT NO. b. PROJECT NO. (DA) 1T262303A308 c. AMC Management Structure Code No. 522C.11.47300 d.	9a. ORIGINATOR'S REPORT NUMBER(S) RR-TR-71-2 9b. OTHER REPORT NO(S) *(Any other numbers that may be assigned this report)* AD_____

10. DISTRIBUTION STATEMENT

Distribution of this document has been approved for public release and sale; its distribution is unlimited.

11. SUPPLEMENTARY NOTES	12. SPONSORING MILITARY ACTIVITY
None	Same as No. 1

13. ABSTRACT

An arc-driven laser suitable for gas-dynamic and similar modes of operation is described. Inversion is obtained by rapid expansion of hot gas mixtures through a supersonic aerodynamic nozzle. Upper vibrational lasing levels are "frozen" at pre-expansion conditions while the lower levels are characterized by conditions in the supersonic flow downstream of the nozzle. A population inversion exists for some distance downstream. Inversion is enhanced by the injection of additives to relax the lower levels at a faster rate. The system is so designed that the gases used, the mixture ratios, and the mass flow rates, as well as the specific enthalpy of the system, may be varied nearly independently. In addition, gases may be injected at various points along the flow, and the results of this feature is stressed.

The laser has been operated under marginal gas-dynamic conditions with all component gases of a CO_2 system premixed prior to expansion. However, most of the work presented deals with the injection of cold CO_2 into the hot supersonic flow mixture immediately downstream of the nozzle throat.

The variation of the 10.6 micron output power, both in magnitude and in space, is presented as a function of the mass flow rate of each component gas. Additional factors, such as input power and upstream pressures and temperatures, are also considered.

It was found that the range of plenum conditions for which lasing may occur is considerably extended in the supersonic mixing mode. In addition, powers more than an order of magnitude higher were obtained with supersonic mixing for the range of available operating conditions.

(Continued)

DD FORM 1 NOV 65 1473 REPLACES DD FORM 1473, 1 JAN 64, WHICH IS OBSOLETE FOR ARMY USE.

UNCLASSIFIED
Security Classification

14 KEY WORDS	LINK A ROLE	LINK A WT	LINK B ROLE	LINK B WT	LINK C ROLE	LINK C WT
Arc-driven laser Supersonic flow Supersonic mixing Output power						

Abstract (Continued)

This report illustrates how parametric studies may be made of various aerodynamic systems. In particular, the effects of controlled amounts of impurities, such as those formed in various combustion processes, may be investigated.

1 April 1971 Report No. RR-TR-71-2

THERMAL LASER EXCITATION BY SUPERSONIC MIXING IN A GAS DYNAMIC NOZZLE

by

H. Lee Pratt

DA Project No. 1T262303A308
AMC Management Structure Code No. 522C.11.47300

DISTRIBUTION OF THIS DOCUMENT HAS BEEN APPROVED FOR PUBLIC RELEASE AND SALE; ITS DISTRIBUTION IS UNLIMITED.

Physical Sciences Directorate
Directorate for Research, Development, Engineering
and Missile Systems Laboratory
US Army Missile Command
Redstone Arsenal, Alabama 35809

ABSTRACT

An arc-driven laser suitable for gas-dynamic and similar modes of operation is described. Inversion is obtained by rapid expansion of hot gas mixtures through a supersonic aerodynamic nozzle. Upper vibrational lasing levels are "frozen" at pre-expansion conditions while the lower levels are characterized by conditions in the supersonic flow downstream of the nozzle. A population inversion exists for some distance downstream. Inversion is enhanced by the injection of additives to relax the lower levels at a faster rate. The system is so designed that the gases used, the mixture ratios, and the mass flow rates, as well as the specific enthalpy of the system, may be varied nearly independently. In addition, gases may be injected at various points along the flow, and the results of this feature is stressed.

The laser has been operated under marginal gas-dynamic conditions with all component gases of a CO_2 system premixed prior to expansion. However, most of the work presented deals with the injection of cold CO_2 into the hot supersonic flow mixture immediately downstream of the nozzle throat.

The variation of the 10.6 micron output power, both in magnitude and in space, is presented as a function of the mass flow rate of each component gas. Additional factors, such as input power and upstream pressures and temperatures, are also considered.

It was found that the range of plenum conditions for which lasing may occur is considerably extended in the supersonic mixing mode. In addition, powers more than an order of magnitude higher were obtained with supersonic mixing for the range of available operating conditions.

This report illustrates how parametric studies may be made of various aerodynamic systems. In particular, the effects of controlled amounts of impurities, such as those formed in various combustion processes, may be investigated.

ACKNOWLEDGMENT

The author is grateful for the advice and assistance of personnel of the Chemical Physics Functions, Physical Sciences Directorate, who helped install and operate the hardware and also participated in the collection of the data. Dr. Thomas G. Roberts provided much of the information concerning the special configuration laser as well as invaluable assistance in organizing and writing this report. Information concerning mass flow rates, as well as information concerning the Army Missile Command plasma facility was obtained in part from Dr. Thomas A. Barr, Jr. Mr. W. LaVaughn Hales and Mr. Charles M. Cason gave assistance in the form of computational aid. Appreciation is especially due Mr. Billie O. Rogers, Mr. Herbert C. Ruge, and Mr. Charles N. Rust who operated and maintained the laser facility.

CONTENTS

		Page
LIST OF ILLUSTRATIONS		vii
CHAPTER 1.	INTRODUCTION	1
	1.1 Background	2
	1.2 Scope of this Work	4
CHAPTER 2.	THEORETICAL CONSIDERATIONS	6
	2.1 N_2-CO_2 Molecular Laser Scheme	6
	2.2 Effects of Additives	8
	2.3 Gas-Dynamic Laser Scheme and Its Advantages	10
	2.4 Thermal Mixing Scheme	13
CHAPTER 3.	EXPERIMENTAL FACILITY	15
	3.1 Power Supply, Control System, and Arc	17
	3.2 Gas Supply and Vacuum Facility	23
	3.3 Laser Components	26
	3.3.1 The Plenum	26
	3.3.2 The Nozzle	32
	3.3.3 The Cavity	32
	3.4 The Assembled Special Configuration Laser	37
CHAPTER 4.	INSTRUMENTATION AND CALIBRATION	42
	4.1 Measurement of Gas Flow Rates	42
	4.1.1 Calibration Procedures	43
	4.1.2 Calculation of Mass and Molar Fractions	46
	4.2 Plenum Temperatures T_o and T_{wall}	47
	4.3 Input Power	48

Page

4.4 Output Power 49

4.4.1 Thermopile Detector System 49

4.4.2 Laser Burn Patterns 50

4.5 Problems Encountered 51

CHAPTER 5. EXPERIMENTAL RESULTS OF GAS-DYNAMIC LASER (MODE I) OPERATION 54

5.1 Maximum Power versus N_2 Flow Rate 54

5.2 Power versus H_2O Flow Rate 56

5.3 Summary of Mode I Operation 56

CHAPTER 6. EXPERIMENTAL RESULTS OF SUPERSONIC MIXING (MODE II) OPERATION 58

6.1 Effects Due to T_{wall} 58

6.2 Power Variation Due to the N_2 Flow Rate 60

6.3 Power Variation Due to the CO_2 Flow Rate ... 63

6.4 Power Variation Due to the He Flow Rate 63

6.5 Power Variation Due to the H_2O Flow Rate ... 69

6.6 Additional Factors Affecting Performance ... 69

6.7 Summary of Mode II Operation 71

CHAPTER 7. DISCUSSION AND RECOMMENDATIONS 72

7.1 Comparison of Modes I and II 72

7.2 Recommendations and Plans for Future Work 73

REFERENCES 75

LIST OF ILLUSTRATIONS

Figure		Page
1	Diagram of Energy Levels of N_2-CO_2 Laser	7
2	Diagram of Gas-Dynamic Laser and Associated Temperatures	11
3	Diagram of Special Configuration Laser	16
4	Photograph of dc Power Generators	18
5	Diagram of Special Configuration Laser Power System	19
6	Diagram of Entire Power and Control System	20
7	Photograph of Control Console	21
8	Diagram of Electric Arc Plasma Generator	22
9	Diagram of Gas Flow System	24
10	Photograph of N_2 Supply	27
11	Photograph of Vacuum Tank and Plasma Facility	28
12	Diagram of Nozzle, Cavity, and Transition Sections	29
13	Diagram of Plenum, Viewed from Above	30
14	Diagram of Plenum, Viewed from Side	31
15	Diagram of Nozzle, Viewed from Downstream	33
16	Diagram of Nozzle, Cutaway View	34
17	Diagram of Cavity, Viewed Along Optical Path	35
18	Diagram of Output Mirror	36
19	Photograph of Special Configuration Laser, Exploded, View 1	38
20	Photograph of Special Configuration Laser, Exploded, View 2	39
21	Photograph of Special Configuration Laser, View 3	40
22	Photograph of Special Configuration Laser, View 4	41

Figure		Page
23	Graph of Output Energy Versus Burn Volume	52
24	Graph of Output Power Versus N_2 Flow Rate (Mode I) ...	55
25	Photograph of Burn Patterns, H_2O Variation (Mode I) ..	57
26	Graph of Output Power Versus T_{wall} (Mode II)	59
27	Graph of Output Power Versus N_2 Flow Rate (Mode II) ..	61
28	Spatial Burn Patterns with N_2 Variation (Mode II)	62
29	Graph of Output Power Versus CO_2 Flow Rate (Mode II) .	64
30	Spatial Burn Patterns with CO_2 Variation (Mode II) A .	65
31	Spatial Burn Patterns with CO_2 Variation (Mode II) B .	66
32	Graph of Output Power Versus He Flow Rate (Mode II) ..	67
33	Spatial Burn Patterns with He Variation (Mode II)	68
34	Spatial Burn Patterns with H_2O Variation (Mode II) ...	70

CHAPTER 1

INTRODUCTION

Since the development of the first working lasers barely a decade ago, considerable time and effort has been expended in the search for higher output laser systems. The possible applications of power lasers are unlimited in the fields of communication, manufacturing, construction, medicine, space exploration, and defense.

Unfortunately many obstacles exist in the attainment of high power systems. Most lasers have a low efficiency. To obtain high power or high energy outputs, considerably more energy must be furnished to the system. If this energy is electrical, then the system cannot have a large average power and still be portable, as is desired in some cases. The relative size, weight, and availability of materials have introduced more obstacles, and the problem of handling a high power beam once it is obtained must also be considered. Then too, many laser schemes are limited in power because of the inherent characteristics of the lasing materials and the reactions taking place.

Despite these obstacles, continuous wave output power has continued to increase from milliwatts, watts, kilowatts, and more recently tens of kilowatts. New lasing materials, methods of producing population inversions, and coupling procedures have been developed. Detectors, mirrors, windows, and other auxiliary equipment have been adapted for the new systems.

One of the more promising areas of work now being studied is the field of gas-dynamic lasing (GDL) systems. Once fully developed, such GDL systems may be able to operate independent of electrical or other external power sources. Bulky and heavy equipment such as vacuum chambers, pumps, and compressors may be eliminated. A portable, high-power, and relatively simple laser may result.

1.1 Background

In 1962-1963 Basov [1] and Hertzberg and Hurle [2,3] reported the possibility of producing population inversion by the heating and cooling of various systems. Inversion is obtained by noting differences in relaxation times for various energy levels during the time thermodynamic equilibrium is being established. Inversion through this means can quite easily be obtained in N_2-CO_2 systems, which have previously produced several kilowatts of laser power [4,5] from glow discharge excitation.

In a typical N_2-CO_2 laser the upper lasing level of the CO_2 is very near the first vibrational level of nitrogen. Energy is pumped into the nitrogen (usually through electron bombardment) to populate this level. By near resonant collisional transfer of energy the excited nitrogen molecules fill the upper CO_2 lasing level, producing a population inversion in the CO_2 molecules.

Gas-dynamic techniques [1-3, 6-22] may also be used to preferentially populate the upper CO_2 level. If the component laser gases are heated and rapidly cooled, the temperature, T_{vib}, associated with the vibrational mode of N_2 remains almost as high as before cooling for an appreciable length of time. However, the time for temperatures associated with the rotational and translational modes to drop is very

short by comparison. Thus a relatively high density of the (v = 1) N_2 state occurs, which selectively excites the upper CO_2 level in collisions.

Several types of rapid, adiabatic cooling systems may be used. Rarefaction waves in shock tubes [10, 17, 23] and chemical shock tubes [10, 24] may be employed. Perhaps the most effective method is the expansion of the gas through a narrow slit [6, 10] or a nozzle [6, 10, 15, 25]. The latter methods are preferred because they provide shorter cooling times and can be operated continuously rather than pulsed.

Several CO_2 GDL systems are now being studied in research programs by AVCO-Everett Research Laboratory [20-22], United Aircraft [16, 19], Ames Research Center [17], and the University of Illinois [12, 14].

The techniques employed in a GDL are not peculiar to a CO_2 laser. Other systems have been treated [6, 10, 13, 19] and much work remains to be done in these fields.

Inversion can be more readily obtained if cold CO_2 is added to the heated N_2 [16, 19]. Selective excitation of the upper lasing level by the excited nitrogen molecules will occur, but initially the lower lasing level will not be populated appreciably by this process. The problem encountered here is that the N_2 and CO_2 must be well mixed to obtain maximum population of the upper lasing level by collisional transfer, but the gases must not be mixed long enough for the lower lasing level to be thermally populated. Systems operating on this principle have been called "thermal mixing" lasers.

If the nozzle in a GDL system is used only to "freeze" the

vibrational levels of N_2, and cold CO_2 is injected into the N_2 flow at various positions relative to the nozzle throat, then a gas-dynamic-thermal mixing laser results. For example supersonic mixing can take place when the CO_2 is injected anywhere downstream of the nozzle throat. Near sonic mixing can be accomplished by injecting cold CO_2 just upstream of the nozzle throat. When operated in this manner, the laser is not a GDL in the ordinary sense and may more appropriately be called a fast flow thermal laser or, as above, a gas-dynamic-thermal mixing laser. Such a laser extends the ordinary operating range of a gas-dynamic laser, as will be shown by the work reported here.

1.2 Scope of This Work

The purpose of this paper is to report the results of operating the same laser system both as a gas-dynamic laser and as a supersonic thermal mixing laser. These experiments were performed utilizing an existing laser facility at the Physical Sciences Laboratory, U. S. Army Missile Command, Redstone Arsenal, Alabama. The facility was designed so that it could be operated in these forms as well as in other forms which include those of some chemical lasers. The system has been named the Special Configuration Laser (SCL) facility.*

An introduction to the theory of gas lasers which exemplifies the characteristics of both GDL and thermal mixing lasers is given in

*Further information concerning the SCL may be found in reports of the following meetings:

Roberts, T. G., Pratt, H. L., Hutcheson, G. J., and Barr, T. A., Jr., "A Versatile Experimental Laser," to be presented in The Laser in Science and Technology conference, University of Washington, Seattle, Washington, date unannounced.

Roberts, T. G., Pratt, H. L., Hutcheson, G. J., and Barr, T. A., Jr., "The Performance of a CO_2 Laser with Supersonic Mixing," Bull. Am. Phys. Soc., 15, 1970, p. 1324.

Chapter 2. The SCL facility is described in Chapter 3 for the configurations used in these experiments. The details of instrumentation and calibration procedures are included in Chapter 4. The results obtained in the GDL mode are presented in Chapter 5, while Chapter 6 includes results obtained in supersonic mixing modes. Finally, comparison of the results obtained in these two modes of operation and recommendations for further work are included in the last chapter.

CHAPTER 2

THEORETICAL CONSIDERATIONS

In this chapter various laser schemes that are relevant to the present work are considered. In particular the N_2-CO_2 laser is discussed, with the laser operating in gas-dynamic, thermal mixing, and similar modes. The effects of additives are considered, with special interest being given to the effects produced by helium and water vapor.

2.1 N_2-CO_2 Molecular Laser Scheme

Figure 1 is a simplified energy level diagram of the CO_2 and N_2 vibrational levels most important in laser operation. CO_2 as the working gas has three vibrational modes corresponding to symmetric stretch, asymmetric stretch, and bending modes. The laser transition takes place between the first excited asymmetric level (00°1) and the first excited symmetric level (10°0). Characteristic radiation is emitted near 10.6 microns in the infrared spectrum. The exact frequencies that are emitted depend upon which sublevels (i.e., rotational energy levels within the vibrational level) are lasing. Transitions follow the selection rule of $\Delta J = \pm 1$, where J is the total angular momentum or rotational quantum number. Generally the line with maximum gain is at or near the P20 transition between the 00°1-10°0 levels.

Nitrogen serves as the carrier or pumping gas. Since N_2 is a homonuclear diatomic molecule, it has no dipole moment, and relaxation

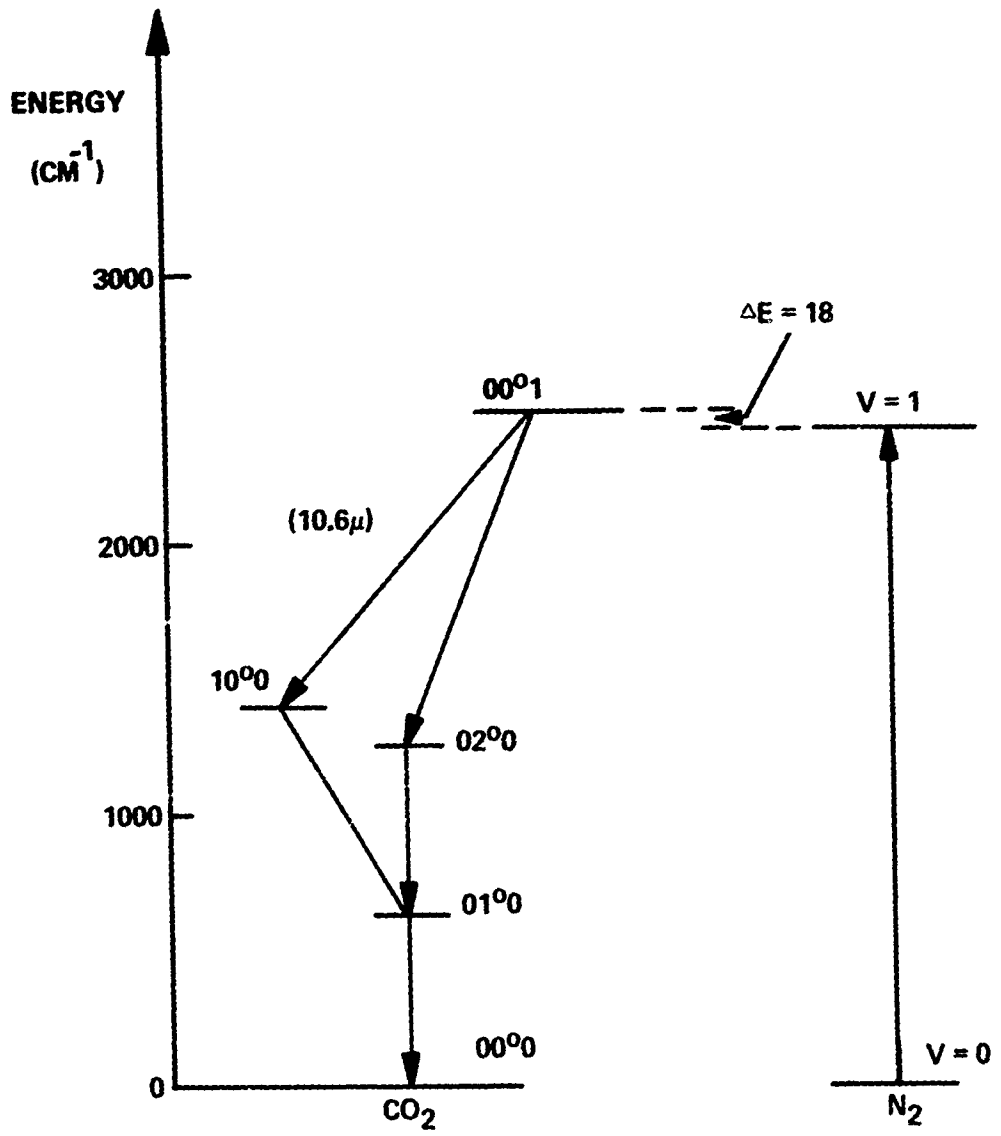

FIGURE 1. DIAGRAM OF ENERGY LEVELS OF N_2-CO_2 LASER

of an excited state cannot occur by dipole radiation. The metastable N_2 therefore has its lifetime controlled by de-activation through collisions with other molecules and the container wall. Furthermore, the first vibrational level (v = 1) of N_2 is very near the upper lasing level of CO_2. The two levels differ in energy only by 18 cm^{-1} as compared to an average thermal energy at room temperature of over 200 cm^{-1}. In other words, $|\Delta E| << kT$ for these two levels, and a near-resonant situation exists between them. Selective excitation of the upper CO_2 level occurs, with N_2 in the first excited state furnishing the required energy.

This is the basic lasing scheme. Various methods may be used to excite the N_2 molecules, such as electron bombardment, heating, etc. A number of techniques may be employed to depopulate the lower lasing levels as quickly as possible. This helps to produce maximum population inversion and allows the CO_2 molecules to be again excited to the 00°1 level for further participation in the lasing process.

2.2 Effects of Additives

Other gases may be added to the N_2-CO_2 laser to improve performance and increase output power. The first continuous wave CO_2 laser [26, 27] operated without the aid of nitrogen, but the effect of nitrogen was soon discovered [28, 29]. The addition of other gases was found in some instances to greatly increase output power. Howe [30] noted that air produced power outputs nearly as high as those with N_2. Howe also found that CO increased the output level.

Witteman [31] noted that a small amount of water vapor added to the system would further raise the output level of a CO_2-N_2 laser,

but that too much water would virtually stop the lasing action. Moeller and Rigden [32] found that a N_2-CO_2-He mixture was far superior to an N_2-CO_2 system. Although Howe [30] had observed that H_2 added to pure CO_2 had no marked effect, Rosenberger [33] obtained improved performance with a N_2-CO_2-H_2 system over a N_2-CO_2 system.

These and certain other additives all tend to produce improved laser performance by creating a greater population inversion among the upper and lower CO_2 lasing levels. The methods of accomplishing this inversion are not the same for each gas and are not fully understood.

It is believed that helium contributes to the inversion in at least three ways: lowering the rotational temperature of the CO_2 and shifting the gain to the lower P branch transitions, increasing the cross relaxation rate so that the populations of adjacent J levels feed the lasing level, and shortening the vibrational lifetime of the lower lasing level. All three factors tend to produce a larger inversion density.

Witteman [34] has noted that the lower vibrational lasing level (10°0) of CO_2 is nearly in resonance with the vibrational level associated with the angle between the O-H bonds in a water molecule. Because of this, only a few collisions with a water molecule are needed to de-excite the CO_2 lower lasing level. In turn the vibrationally excited water molecule relaxes to translational motion when colliding with other water molecules. Perhaps the dominant effect of H_2O is to depopulate the lower lasing level. It also has some effect on the upper CO_2 or N_2 levels, since too much water decreases lasing action. (Most additives do have an optimum mixing ratio, which if exceeded either decrease or do not change the laser performance.) H_2 has an effect

similar to that of H_2O, perhaps due to the water created in the system, as well as other influences.

In a system where power is extracted over a certain distance along the flow, additives may prove to be a hindrance. For example, in the SCL, where power is extracted over a limited portion of the flow, helium decreases the total output power which can be obtained. This effect will be discussed later.

2.3 Gas-Dynamic Laser Scheme and Its Advantages

Several factors must be considered in deciding which laser system is best suited for a particular purpose. A laser of high efficiency may be desired, but the same system may have an output level that is too low. Power is not the only important factor, since most systems may be made larger to produce more power. An important parameter may be energy (or power) per cavity length or volume. In the case of a flowing system, a useful figure of merit may be output power per mass flow rate. Cost, simplicity, reliability, size, mobility, and power requirements must also be considered.

A gas-dynamic laser shows promise of meeting several of these criteria perhaps better than other systems. Figure 2 is a diagram of a GDL CO_2 system under typical conditions. The top portion is a cross-section of the plenum, nozzle, and cavity sections. Upstream or stagnation conditions are denoted by the zero subscript. An asterisk denotes conditions at the nozzle throat. Conditions downstream in the cavity region are indicated by the symbol for infinity. The lower portion of the figure is an idealized plot of temperatures as a function of distance in the flow direction.

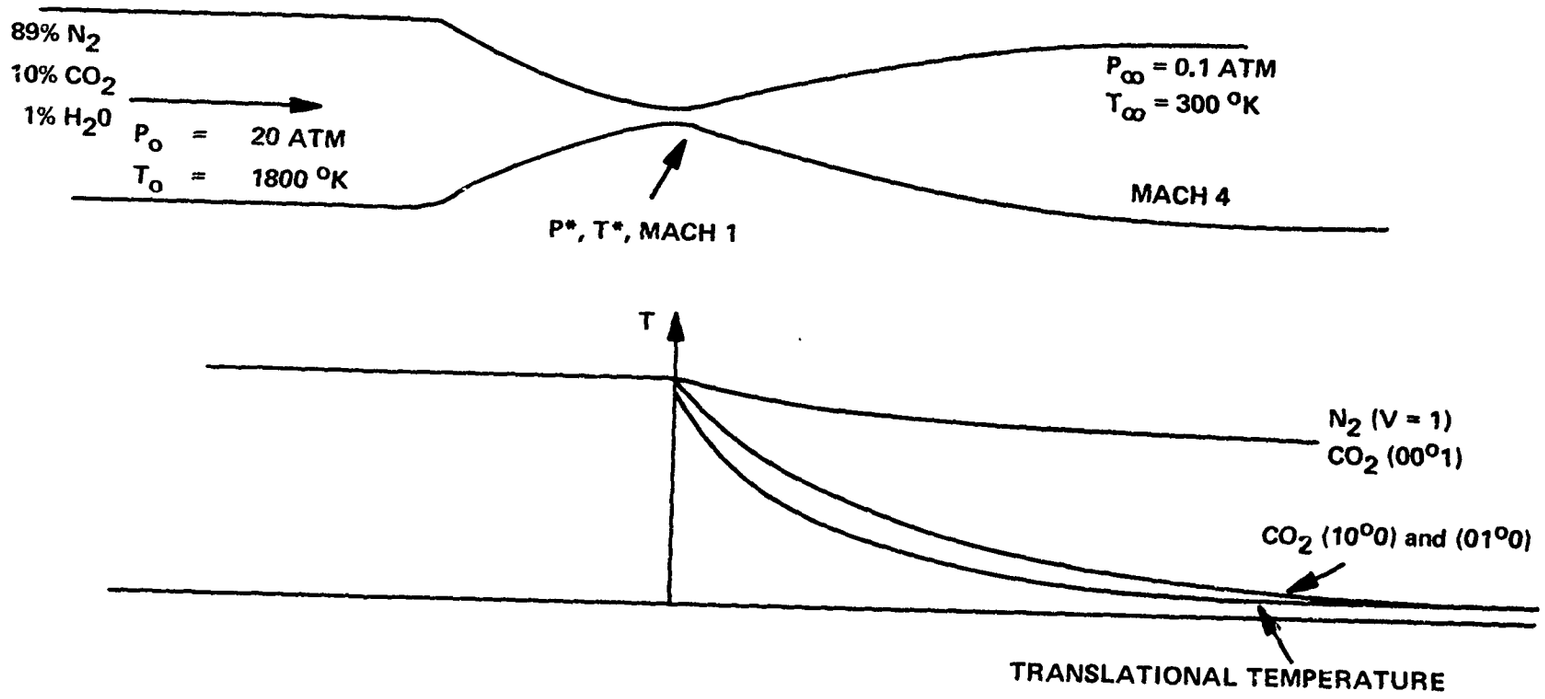

FIGURE 2. DIAGRAM OF GAS-DYNAMIC LASER AND ASSOCIATED TEMPERATURES

In the upstream region the gas mixture is in thermal equilibrium at a high temperature and pressure. The gas is then rapidly expanded through a supersonic nozzle. A high Mach number and low pressure results. Temperatures associated with translational and rotational energies rapidly drop to the free stream temperature. The population of the 10°0 and 01°0 levels of CO_2 also drop quite rapidly to the freestream value. The upper lasing level (00°1) of CO_2 and the excited N_2 levels have a slower vibrational relaxation rate and the temperature associated with the upper lasing level remains nearly as high as before expansion. That is, the population of this level remains about the same. The level is said to be "frozen" at this temperature and density. Since the population of a level is proportional to its vibrational temperature, an inversion exists when the difference in the vibrational temperatures is large enough. Once achieved, a population inversion may exist for a considerable distance downstream. Depending upon the configuration and flow parameters, inversion may exist for a distance of less than a centimeter from the throat to perhaps a meter downstream. A portion or all of this region may be equipped with mirrors and a method of coupling out part of the beam.

An important feature of the GDL is the fact that the gas mixture is in equilibrium at the plenum. It does not matter how these conditions were formed. An arc heater, chemical combustion, or other source of heat may be utilized. Ideally, this source would be independent of electrical power. Then too, the gas flow may be exhausted either into a vacuum chamber or into the atmosphere when the device is fitted with a proper diffusor. Continuous wave power up to 60 kilowatts have been reported from these devices [21, 22]. The GDL shows

promise of being quite useful as a source of high power laser energy.

2.4 Thermal Mixing Scheme

For proper gas-dynamic operation, the nozzle configuration must be fairly well optimized. Gas properties such as mixture ratios, pressures, and temperatures must also lie within a certain range. The upper level of N_2 must be frozen, but the lower CO_2 level must be allowed to relax during expansion.

Inversion can be more readily obtained if some of these requirements are removed. For example, if cold CO_2 is used, then the lower CO_2 level need not be relaxed and it is necessary only to freeze the upper level of N_2. The CO_2 molecules will be selectively excited to the upper level as previously mentioned. This can be accomplished if the CO_2 is injected into the hot N_2 at a point further downstream. If, cold CO_2 is injected downstream of the throat, it will be mixing with the N_2 supersonically. The CO_2 may also be mixed immediately upstream of the throat in the near-sonic region.

Such thermal mixing schemes all have as their basic objective to produce maximum inversion of the CO_2 states. The upper CO_2 level will become most populated by mixing upstream as far as possible. The lower lasing level will remain deplenished only if mixing occurs very near to the optical cavity. Therefore, to produce optimum inversion, the point at which mixing occurs must be a compromise between these two incompatible conditions.

In the work reported here, both GDL and supersonic mixing schemes were employed. A very short period of time was devoted to the near-sonic mixing scheme. Promising results were obtained, but the

aerodynamics of the nozzle were such that the results cannot be compared to the other modes of operation.

CHAPTER 3

EXPERIMENTAL FACILITY

The SCL (Figure 3) utilizes an optical cavity with inside dimensions approximately 1.5 x 6 x 12 inches. Through it the component gases of the carbon dioxide laser flow at hypersonic velocities. Hot nitrogen, obtained from an electric arc plasma generator, is swept through a 1.5 x 2 x 12 inch nozzle into the cavity. Carbon dioxide and other gases are either premixed through sonic orifices or mixed upon injection into the plenum upstream from the nozzle. Injection ports enable additional gases to be injected into the flow downstream of the nozzle throat. After being used in the optical cavity the gases are exhausted into a 1500 cubic foot vacuum tank. Power for the arc generator is obtained from two dc generators, each rated at 575 volts and 2250 amperes.

Power, control, and vacuum components for the SCL are obtained by utilizing portions of the Army Missile Command 8000 kilowatt Plasma Facility [35, 36]. This facility is a general-purpose low temperature plasma device ($T \approx 5000°$ to $10,000°K$) and has been operated primarily as a hyperthermal blowdown wind tunnel for reentry simulation of IRBM's and ICBM's in certain altitude regions. Two of the facility's six dc generators, one arc identical to those of the test facility and a portion of the control system and vacuum chamber have been adapted for the SCL work.

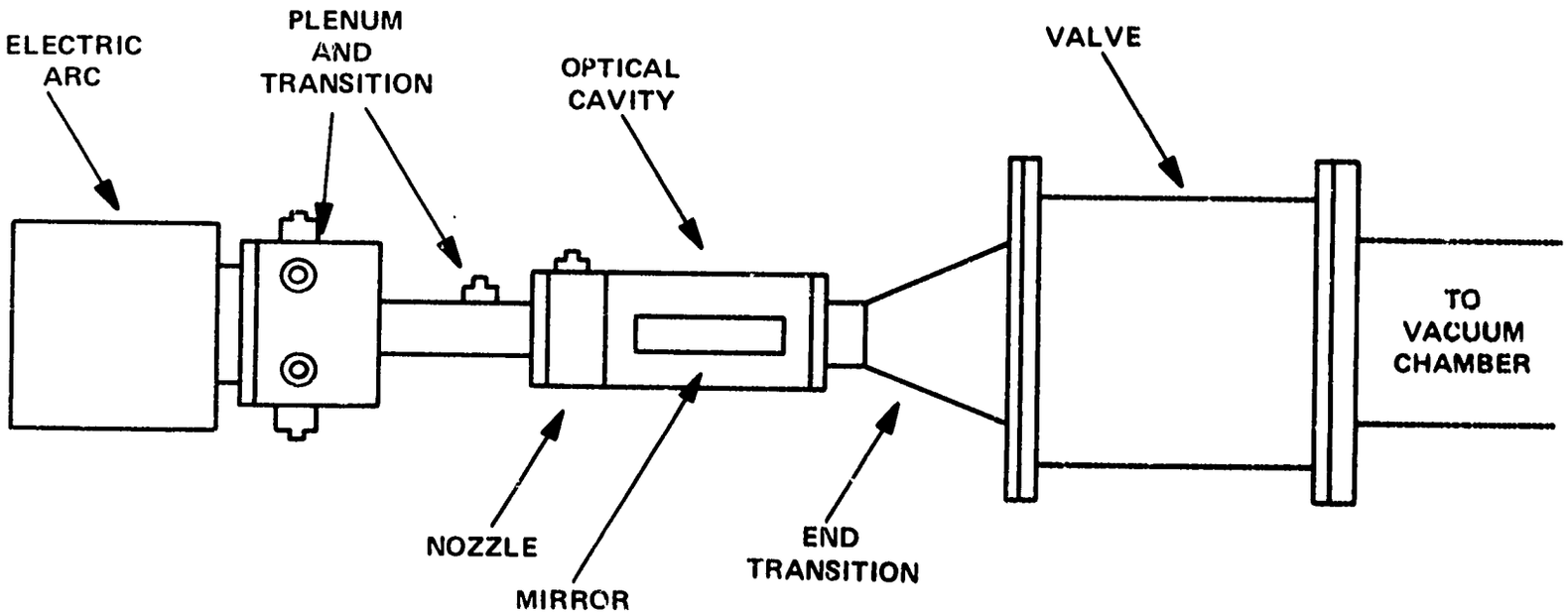

FIGURE 3. DIAGRAM OF SPECIAL CONFIGURATION LASER

3.1 Power Supply, Control System, and Arc

Power is obtained from the local high voltage three phase ac distribution system. 44,000 volts of three phase ac is stepped down by a local substation to 4160 volts of three phase ac (nominal 8000 kW). This voltage is distributed to three synchronous drive motors with a nominal power rating of 1500 horsepower. Each motor drives two 575 volt, 2250 ampere dc generators on a common shaft (Figure 4). For the SCL, two generators are wired in series (Figure 5) to double the range of the applied voltage to the arc. This allows required voltage and current levels to be reached without pushing one generator near its limits. The typical operating level is near 1 megawatt of power to the arc but lower and higher power levels have been used.

The power installation also includes rotary and solid-state exciters for the field windings of the motors and generators. The generators are driven at a constant speed and the output is regulated by varying the field excitation. Six 65 kilowatt, three phase, phase-controlled thyristor amplifiers regulate the field currents of the generators (Figure 6). Control and digital multiplexing components, together with overload protection complete the power supply. All functions are monitored and operated from a single console (Figure 7). The power control system may be used in a feedback circuit with the plenum pressure controlling the arc current, or with an external programmed reference current providing feedback, or with no feedback. (So far the SCL has been operated with no feedback from the laser proper, although feedback may be included if desired.)

The electric arc plasma generator, designed by Mayo, Wallio, and Wells [36] is shown in Figure 8. When operated on the SCL, the

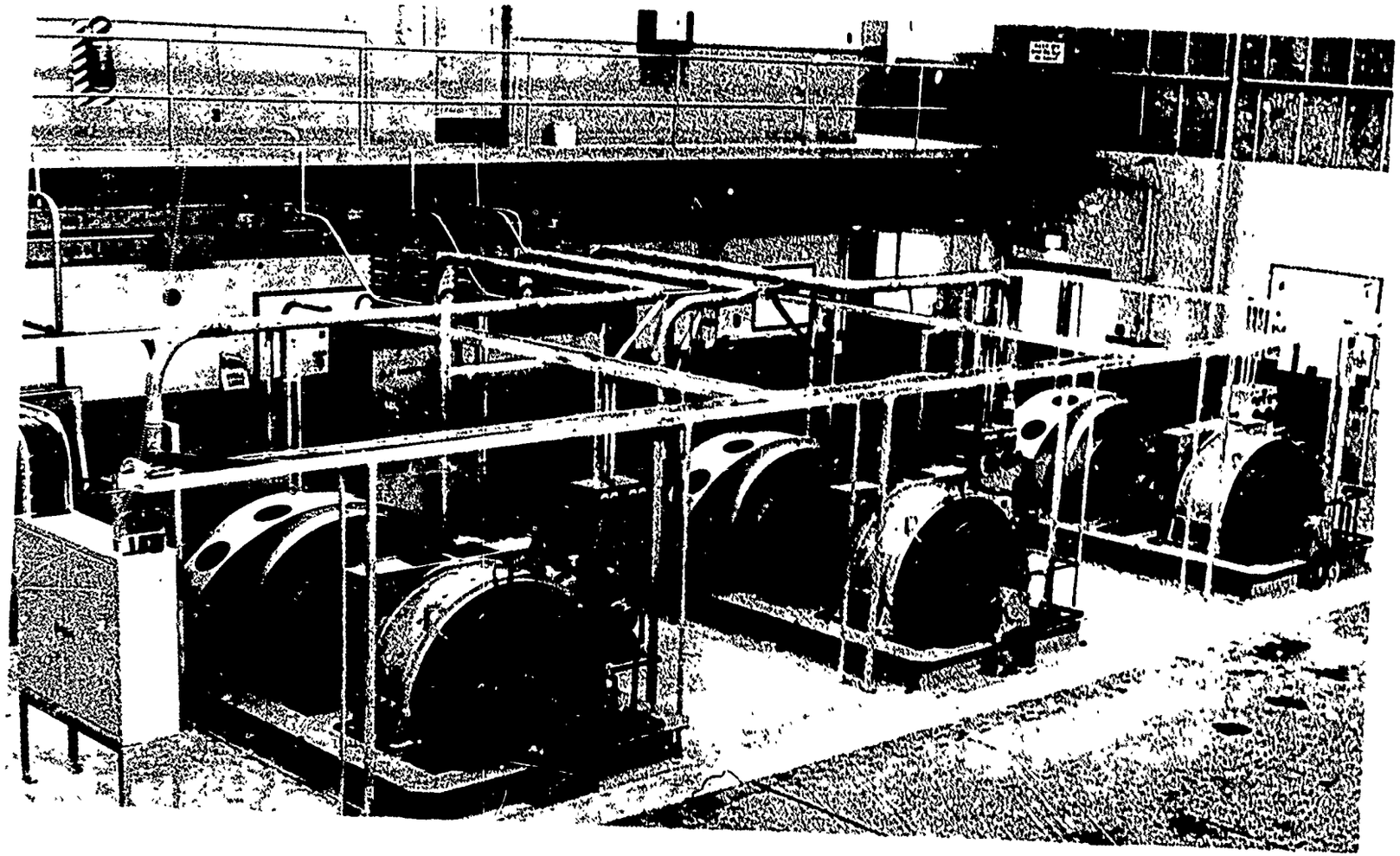

FIGURE 4. PHOTOGRAPH OF dc POWER GENERATORS

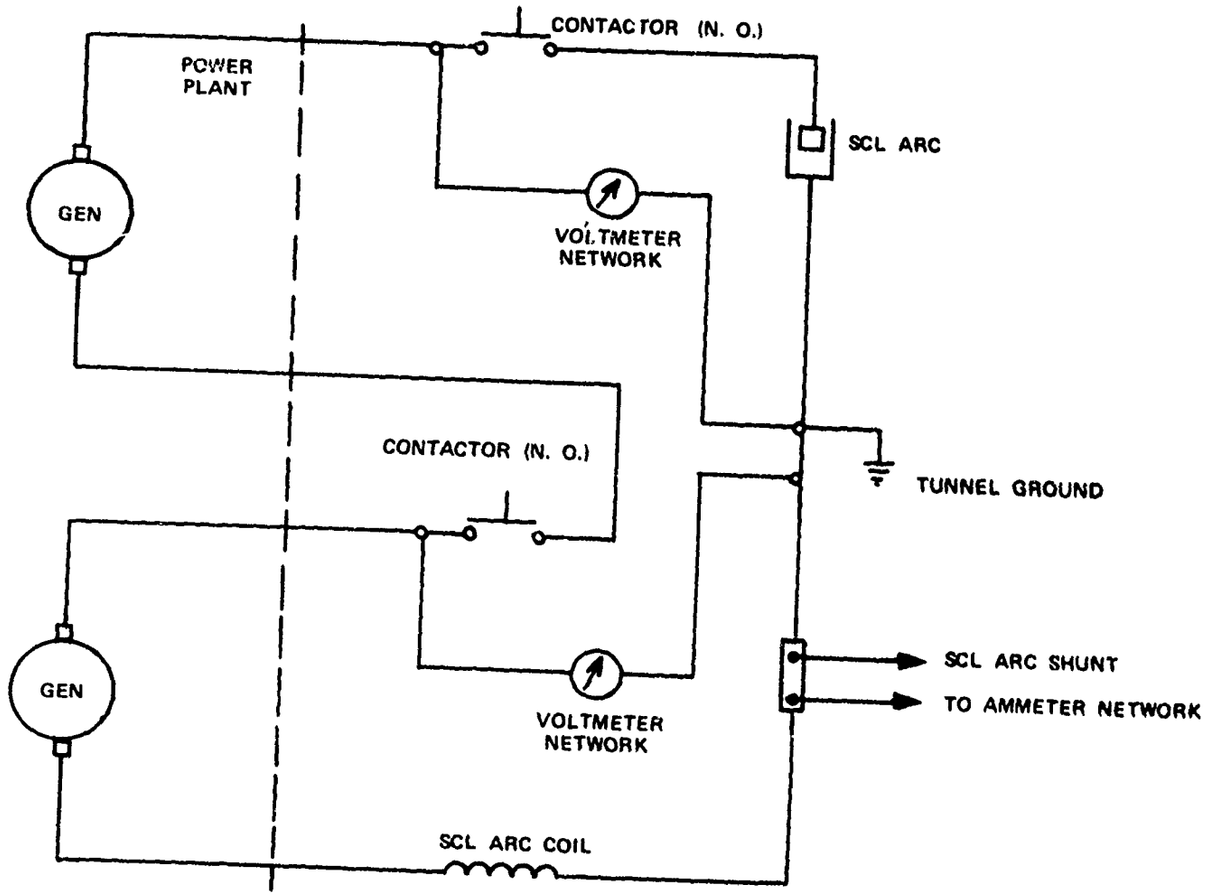

FIGURE 5. DIAGRAM OF SPECIAL CONFIGURATION LASER POWER SYSTEM

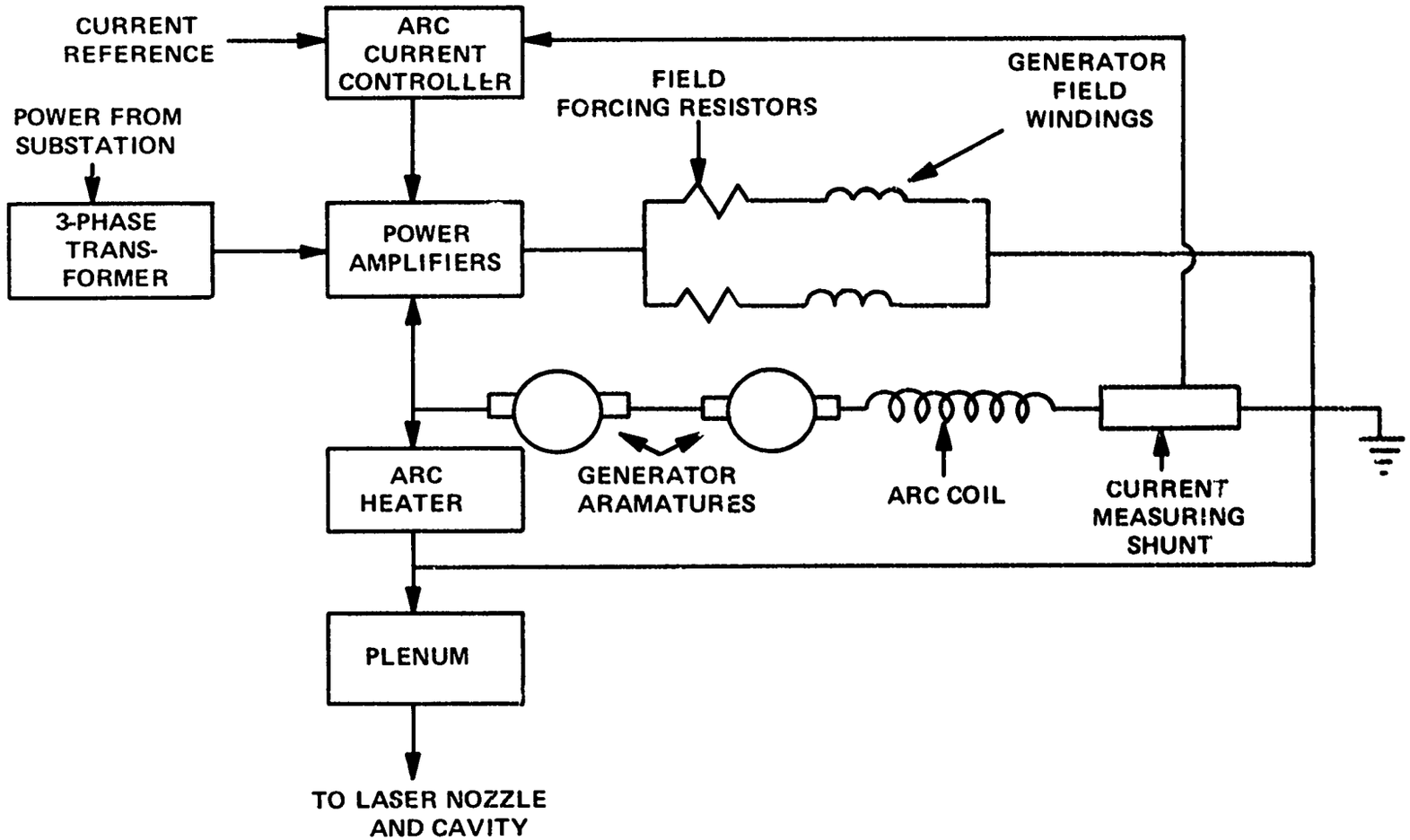

FIGURE 6. DIAGRAM OF ENTIRE POWER AND CONTROL SYSTEM

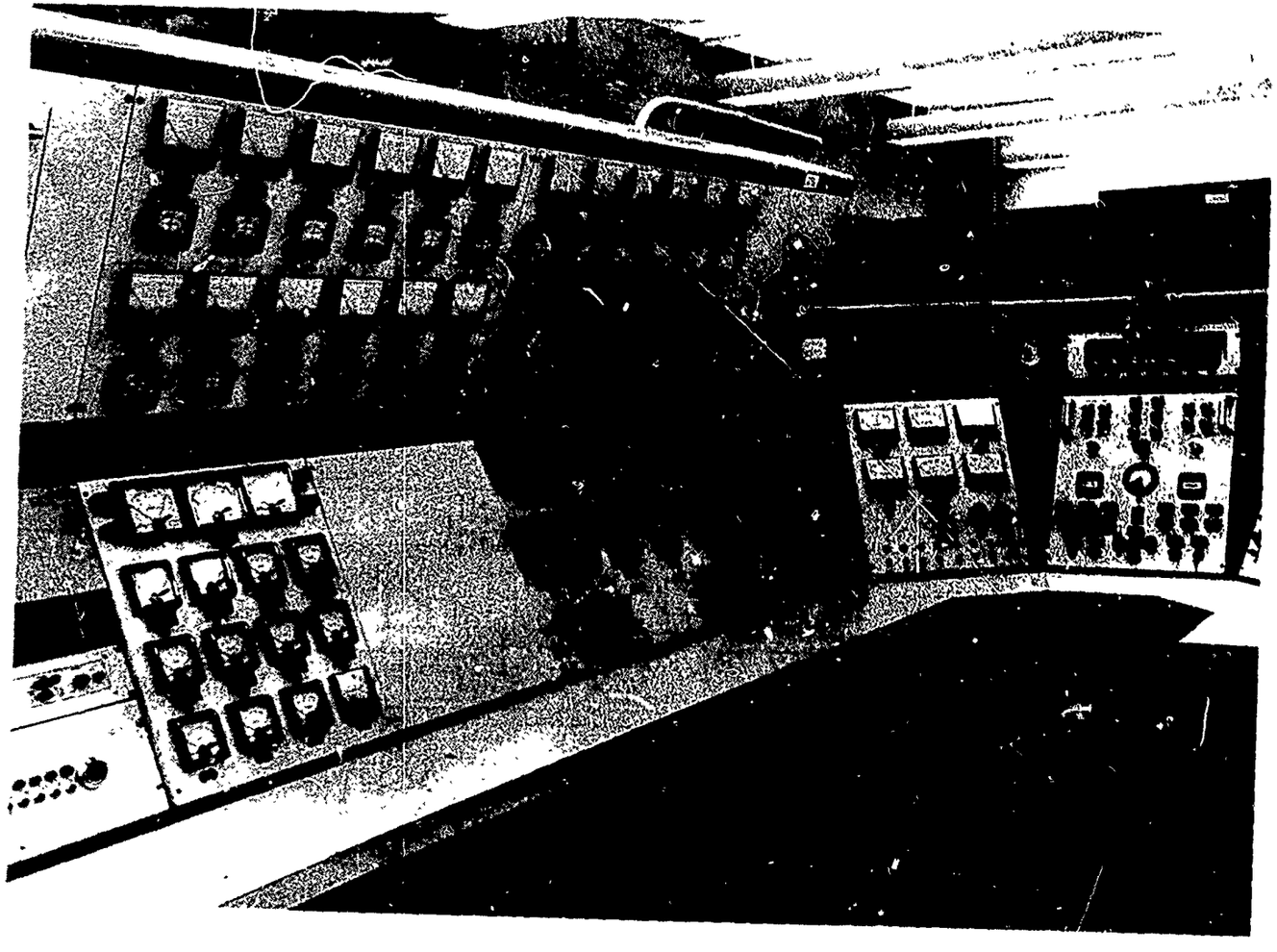

FIGURE 7. PHOTOGRAPH OF CONTROL CONSOLE

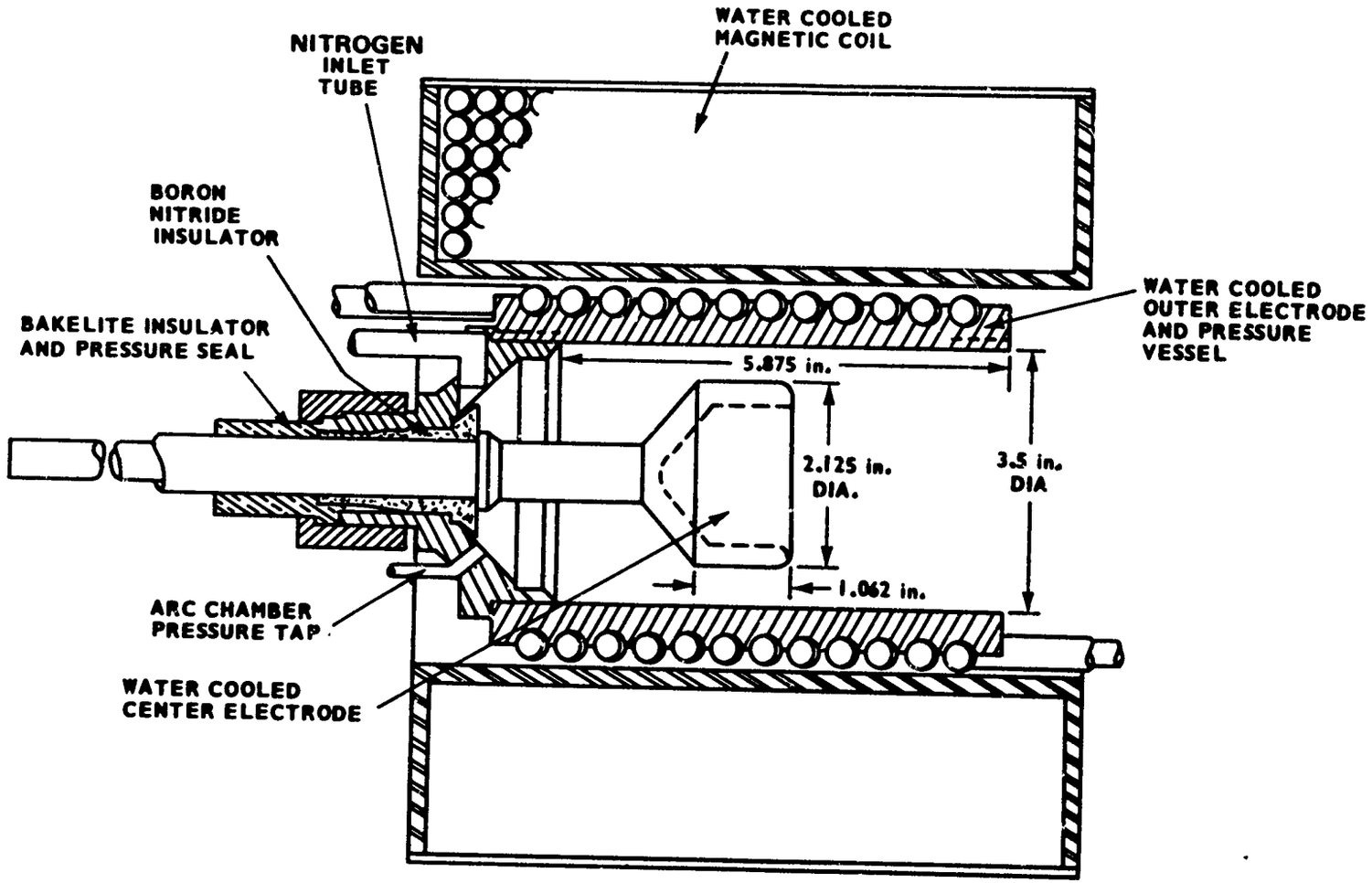

FIGURE 8. DIAGRAM OF ELECTRIC ARC PLASMA GENERATOR

arc is used to heat N_2 instead of air. The generator is so designed that the strong solenoidal magnetic field (0.07 w/amp) causes the arc to rotate rapidly around the anode in the gap. This design tends to reduce overheating and evaporation of the electrode surfaces, increase the voltage of the arc for a given current, improve electrical stability, and decrease electrical noise and pressure fluctuation. The arc is ignited by a spark plug system [37]. The spark plug arc produces a small tongue of plasma which initiates the main arc in the electrode gap. Water at 300 to 500 psig is used to cool the arc and a shunt for measuring current. Conductors running from the dc generators to the arc heater are made of 500-MCM copper cables. Suitable contactors (Square D Class 8502, Type GG 1) are used to switch the main power leads to the arc.

3.2 Gas Supply and Vacuum Facility

Figure 9 is a diagram of the SCL's gas flow system. All hand regulators and manual valves are preset before the laser is operated. Air actuated valves and solenoid valves may be controlled manually at the SCL for test purposes. During an actual power run, however, they are controlled at the main power supply console (Figure 7). The entire system is operated remotely because of safety precautions.

Only a portion of the N_2 supply is passed through the arc. The rest of the N_2 and other gases are injected into the plenum as diluents. The diluents are heated by the hot N_2 from the arc and this produces the equilibrium conditions in the plenum prior to expansion through the nozzle. The mass flow rates of all the gases are controlled by the use of sonic orifices. When the gases are premixed

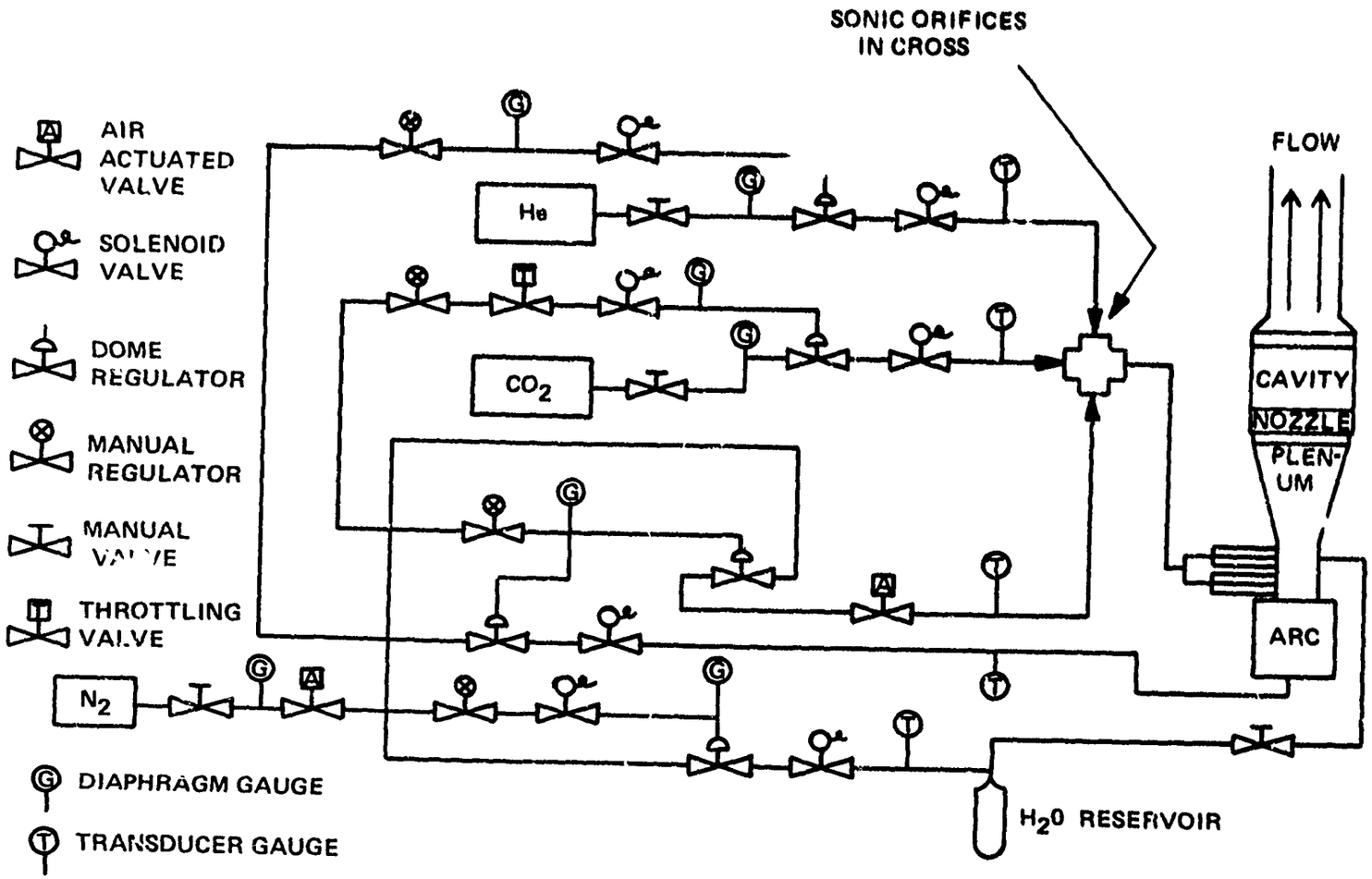

FIGURE 9. DIAGRAM OF GAS FLOW SYSTEM

before injection into the plenum as diluents for GDL type operation, the system is said to be operating in "Mode I." If cold CO_2 is injected downstream of the nozzle throat for supersonic mixing, then the system is said to be operating in "Mode II."

Water may also be injected into the plenum through one of the plenum lines while operating in either mode. The water flow rate is controlled by setting the nitrogen back pressure and upon reaching the plenum the liquid state is changed to vapor and mixed with the other component gases.

N_2, CO_2, He, and H_2O are the gases most often used, but any one or several gases may be eliminated from the system at any time, and additional additives may be included. The SCL lends itself quite readily to parametric studies of the effects of additives on the operation of gas dynamic or similar laser systems.

Again referring to Figure 9, standard components for gas handling are employed. The dome regulators are manufactured by Grove Valve and Regulator Company, and Models 94 W and BX 205 N2 are used. The solenoid valves are Marotta Models MV 74 and MV 140. The air valves are Worthington Controls Model 3620. For the hand regulators, Tescom multiple range Flo-tron regulators, Model 26-1025-34 are used. Various manual valves are used depending upon required flow rates.

Figure 9 shows the SCL flow chart for Mode I operation. In this mode, N_2, CO_2, and He are mixed in a cross fitted with sonic orifices for each component gas. The sizes of the orifices together with gas pressures determine the flow rate of each gas. (This is discussed further in Chapter 4.) The premixed gases are then fed into the plenum through six lines or five lines with H_2O being injected

through the sixth line. In mode II operation the CO_2 line is disconnected from the cross and connected to the downstream side of the nozzle.

Commercial grade gases are used with He and CO_2 supplied from standard size gas bottles. Because of the much larger requirements for N_2, this gas is obtained from a special tank (Figure 10).

The vacuum facility includes a 13,550 cubic foot vacuum chamber (Figure 11). However, only a portion, 1550 cubic feet, of the vacuum chamber is normally used for the SCL. Pumping is obtained by a 300 cfm Stokes Microvac pump, Model 412 H-10, with a Roots booster pump, type RGS-SP-AVM, size 615. A Texas Instruments fused quartz precision pressure gauge, Model 141, monitors the vacuum tank pressure.

3.3 Laser Components

In addition to the arc and vacuum system, the SCL has three primary parts: plenum, nozzle, and cavity (Figures 3 and 12). Transition sections from the plenum to the nozzle and from the cavity to the vacuum tank valve enable the three sections to be coupled together and connected to the arc and the vacuum tank. The hardware is made of stainless steel, fitted with appropriate gaskets for bolting together.

3.3.1 The Plenum

Located between the arc and the nozzle, the plenum (Figures 13 and 14) serves as a mixing chamber for the component gases. Hot N_2 from the arc and the premixed cold gases are combined and allowed to reach thermodynamic equilibrium in this section before expansion through the nozzle and into the cavity. H_2O may also be injected into the system at this point. Thermocouples and pressure transducers measure

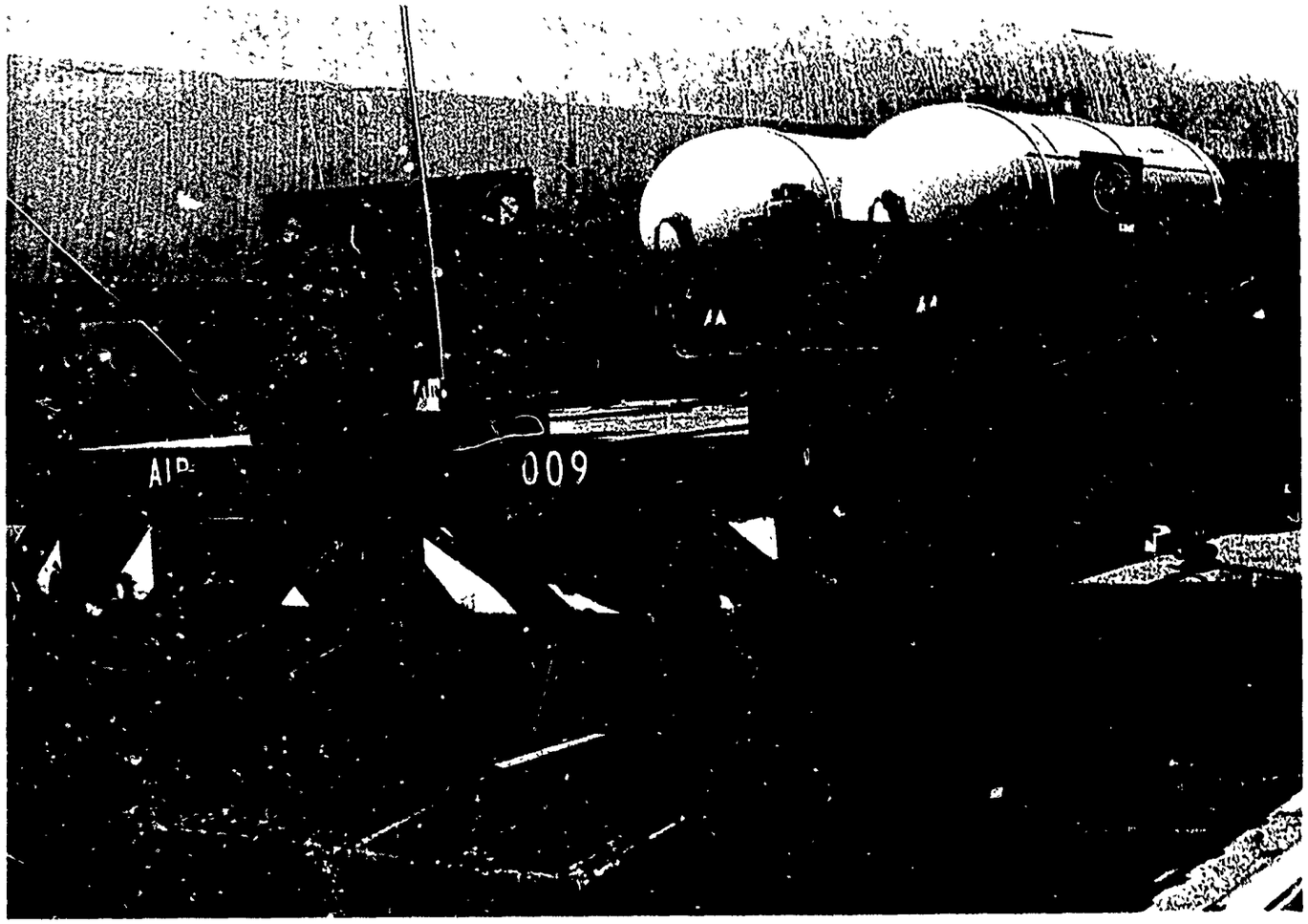

FIGURE 10. PHOTOGRAPH OF N_2 SUPPLY

FIGURE 11. PHOTOGRAPH OF VACUUM TANK AND PLASMA FACILITY

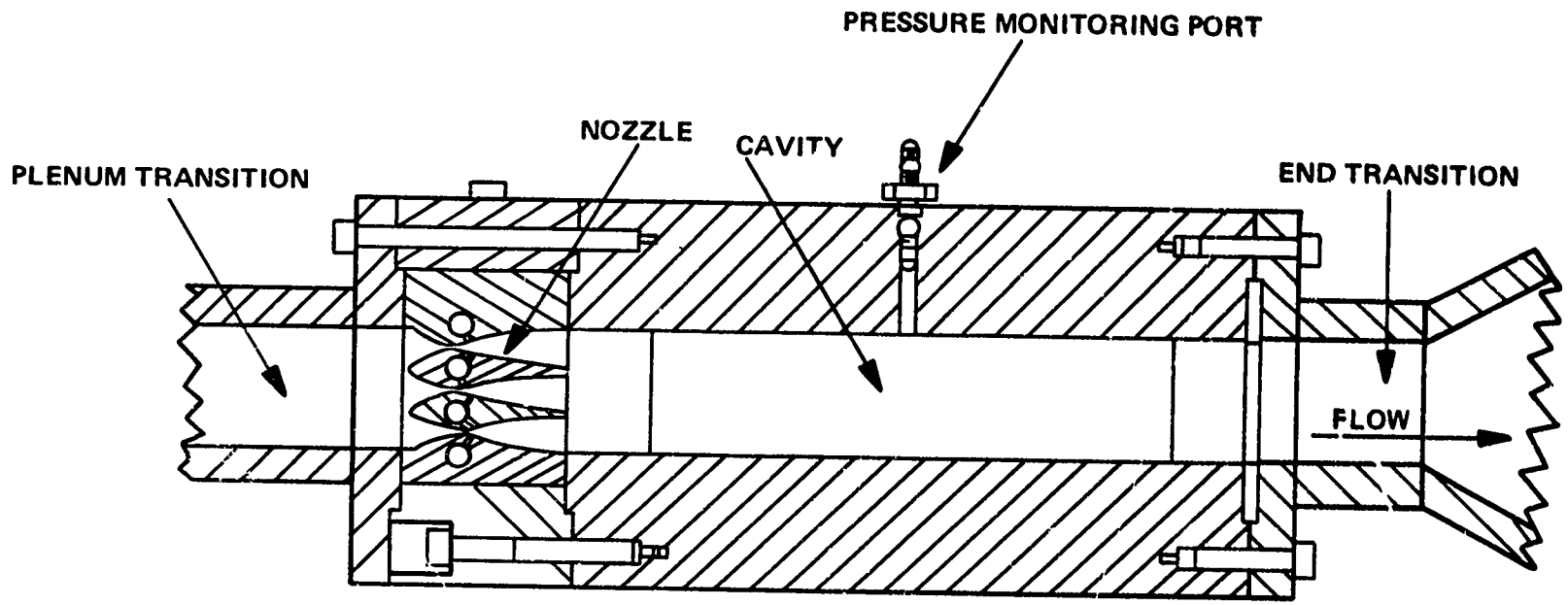

FIGURE 12. DIAGRAM OF NOZZLE, CAVITY, AND TRANSITION SECTIONS

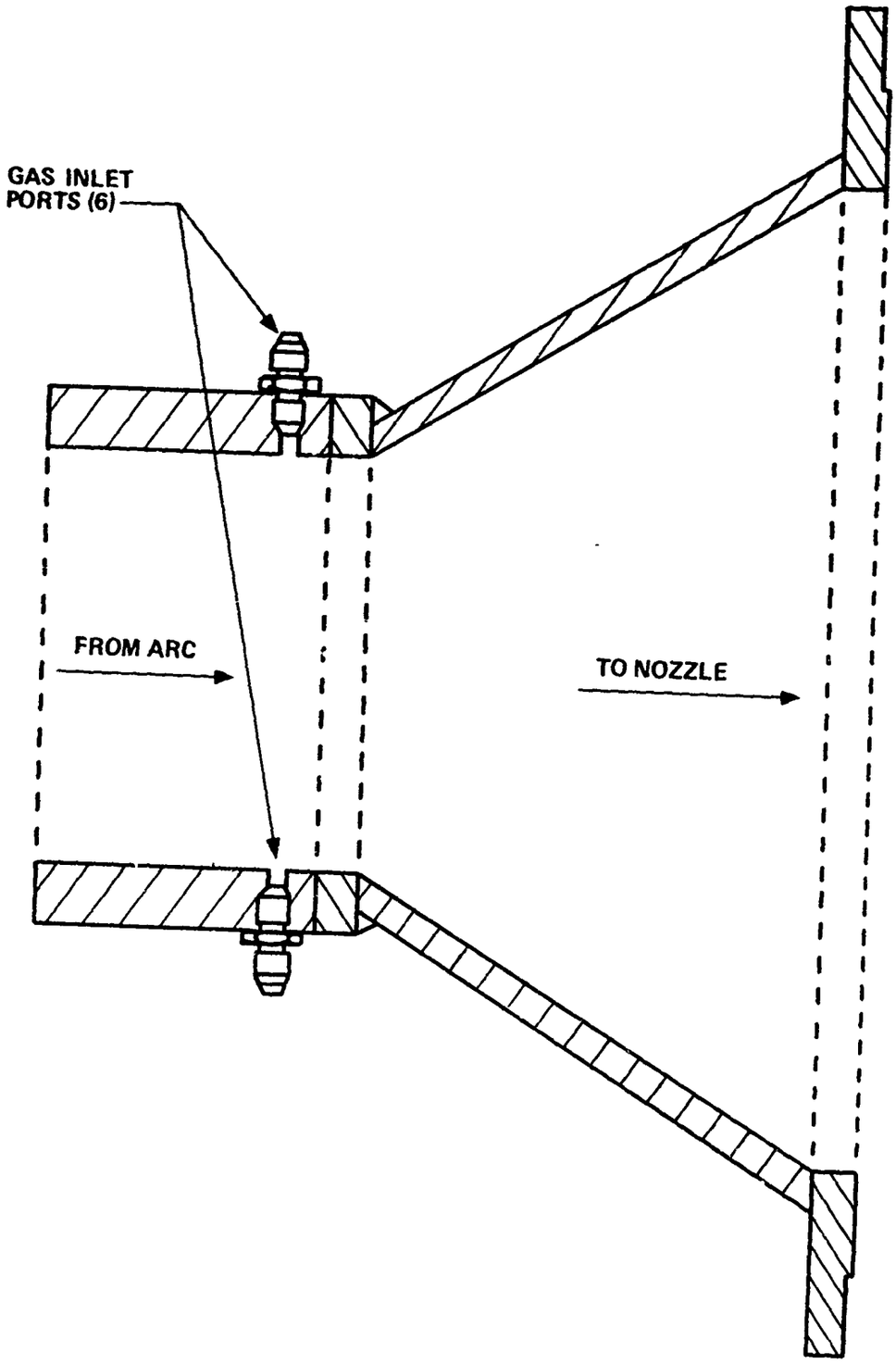

FIGURE 13. DIAGRAM OF PLENUM, VIEWED FROM ABOVE

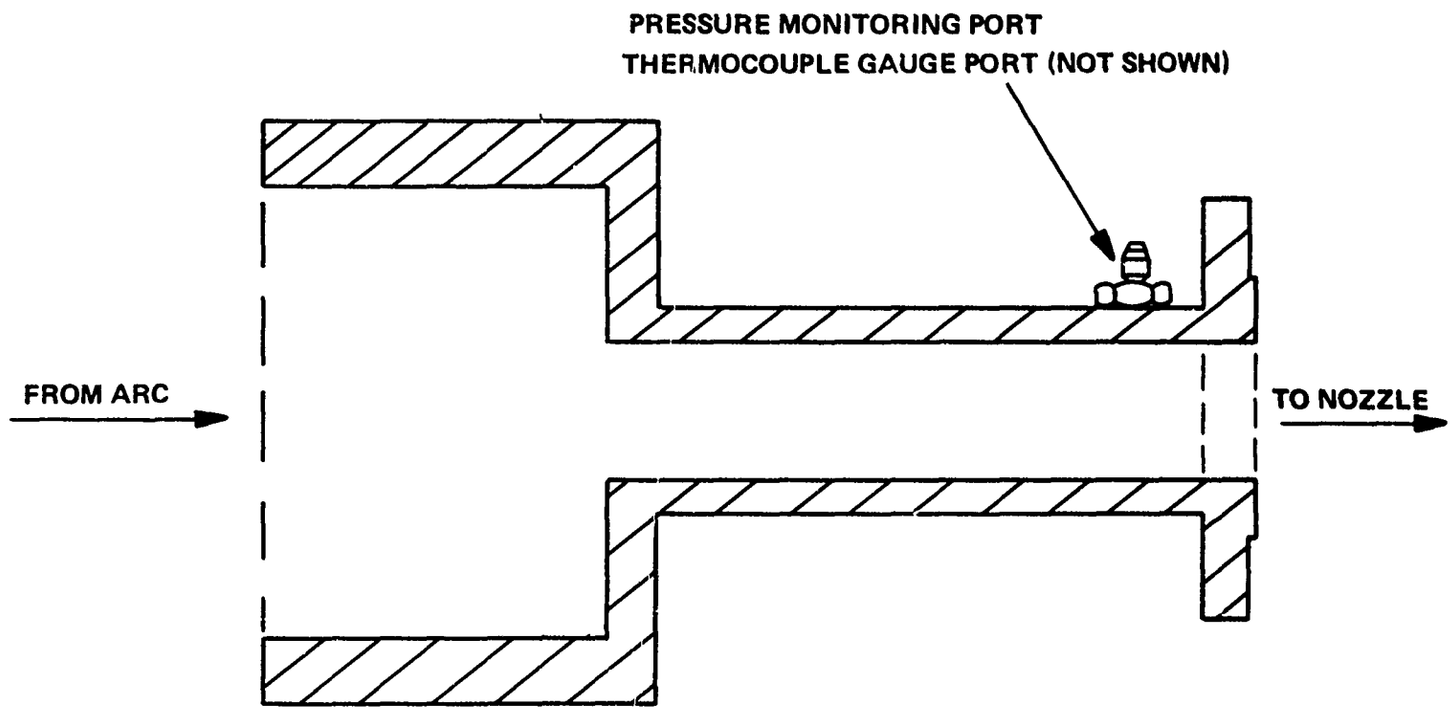

FIGURE 14. DIAGRAM OF PLENUM, VIEWED FROM SIDE

the temperature and pressure just before the gas mixture reaches the nozzle.

3.3.2 The Nozzle

Figures 15 and 16 show the nozzle. The actual working area of the nozzle is approximately 12 inches wide and 1.5 inches high, the nozzle being 2 inches long. The distance from the throat to the nozzle exit is 1.26 inches. The throat height is 0.032 inch. As seen in the diagrams there are three narrow slits for gas flow. Six rows of 0.030-inch holes, two rows in each slit, are located downstream of the throat and enable CO_2 to be injected into the system for Mode II operation. Each of the six rows contains sixty holes along the width of the nozzle. The CO_2 enters the nozzle through two ports in the top cap. Other nozzle configurations have been used, but only this nozzle was employed in the work reported here. Information for the nozzle contour was obtained from the AVCO-Everett Research Laboratory.

3.3.3 The Cavity

Figures 12 and 17 show the optical cavity. Figure 12 views the cavity along the flow path with the plenum and nozzle in place. Figure 17 views the cavity perpendicular to the flow, along the optical path. The distance between the mirrors is approximately 12 inches, with the mirrors forming part of the flow channel. The mirrors are gold plated optically flat pieces of copper, aluminum, or stainless steel. 181 holes (0.039 inch in diameter) in one of the mirrors enable power to be extracted from the cavity at a distance of more than 5 inches along the flow (Figure 18). The upstream edge of the mirror is 2.3 inches from the throat, while the first output holes are 2.9 inches

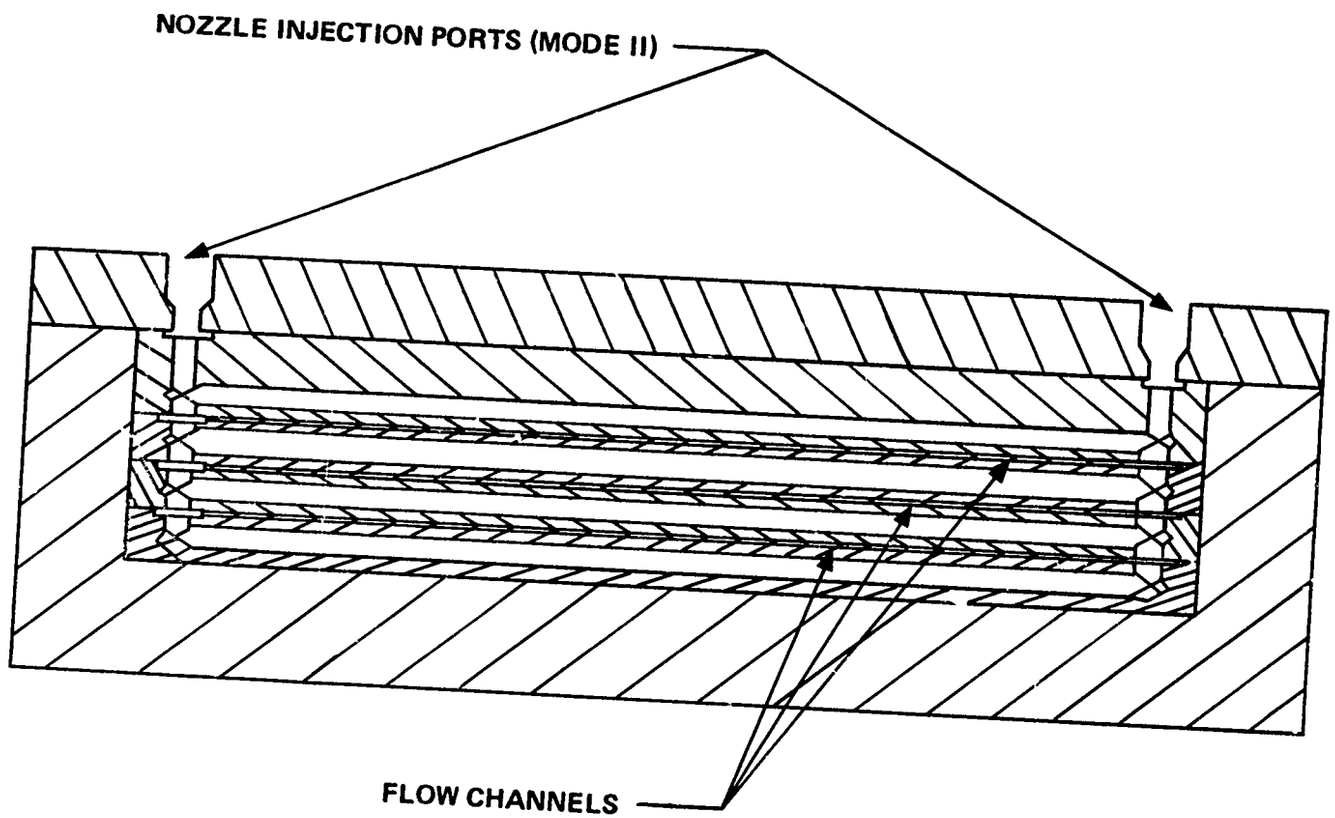

FIGURE 15. DIAGRAM OF NOZZLE, VIEWED FROM DOWNSTREAM

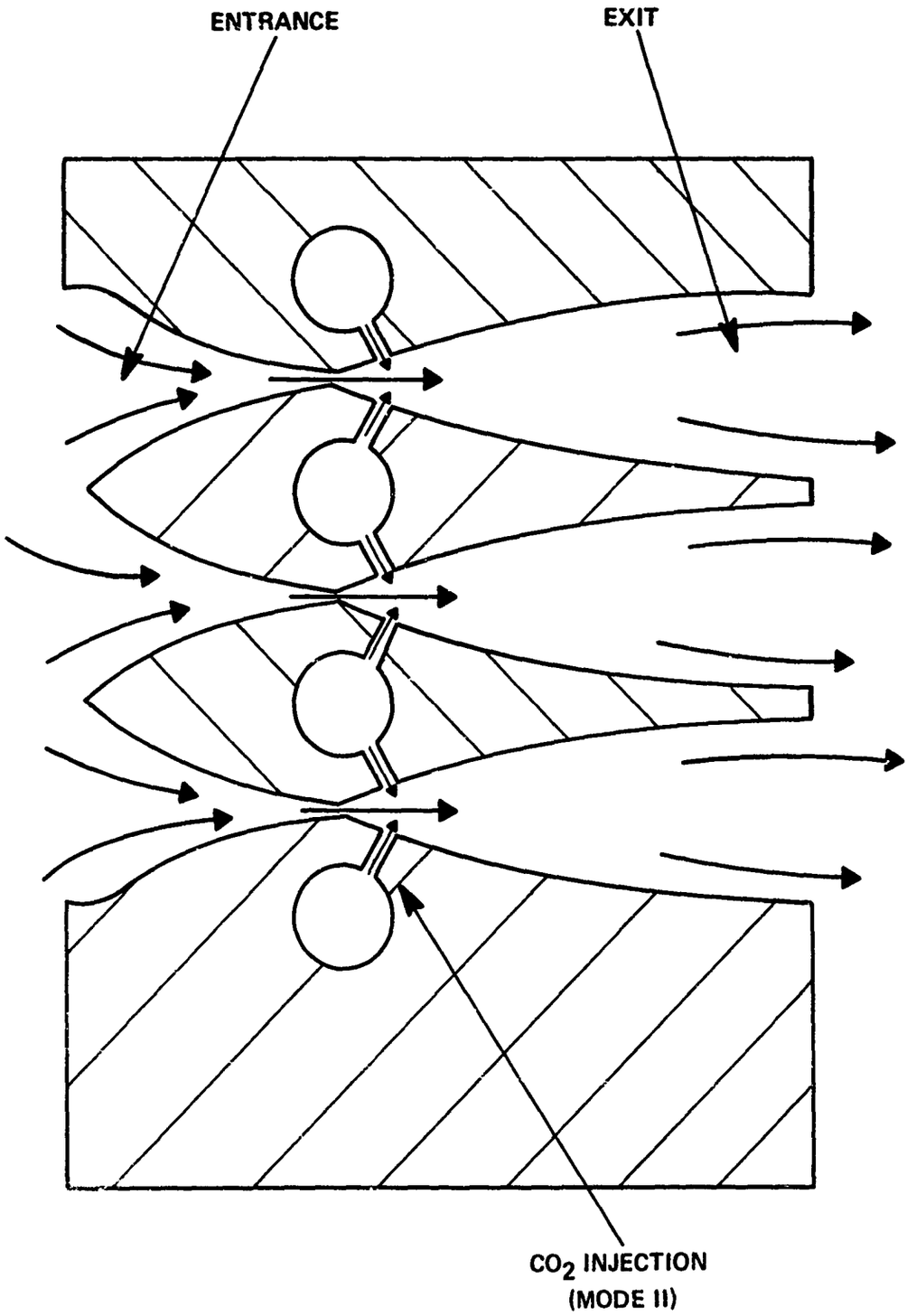

FIGURE 16. DIAGRAM OF NOZZLE, CUTAWAY VIEW

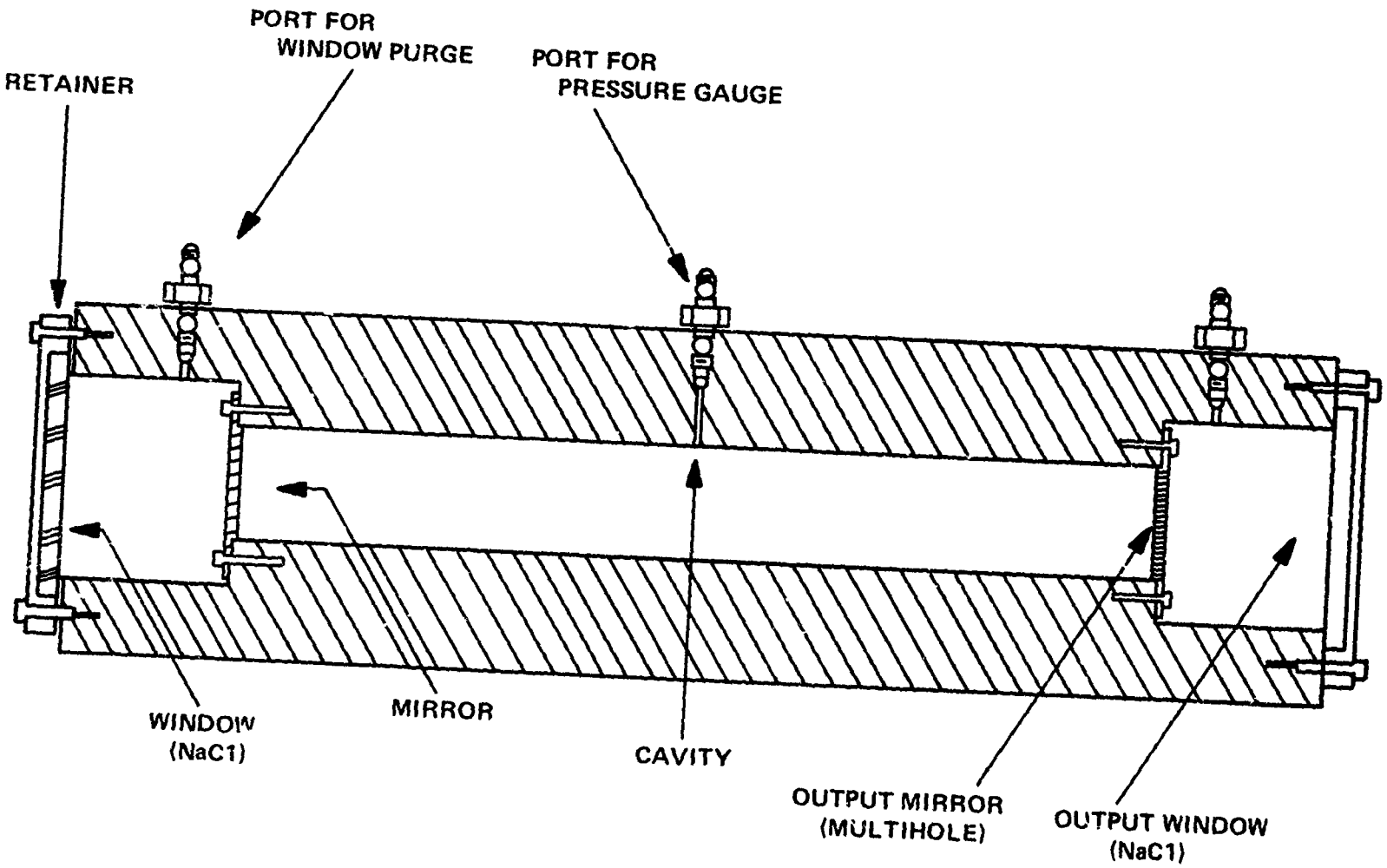

FIGURE 17. DIAGRAM OF CAVITY, VIEWED ALONG OPTICAL PATH

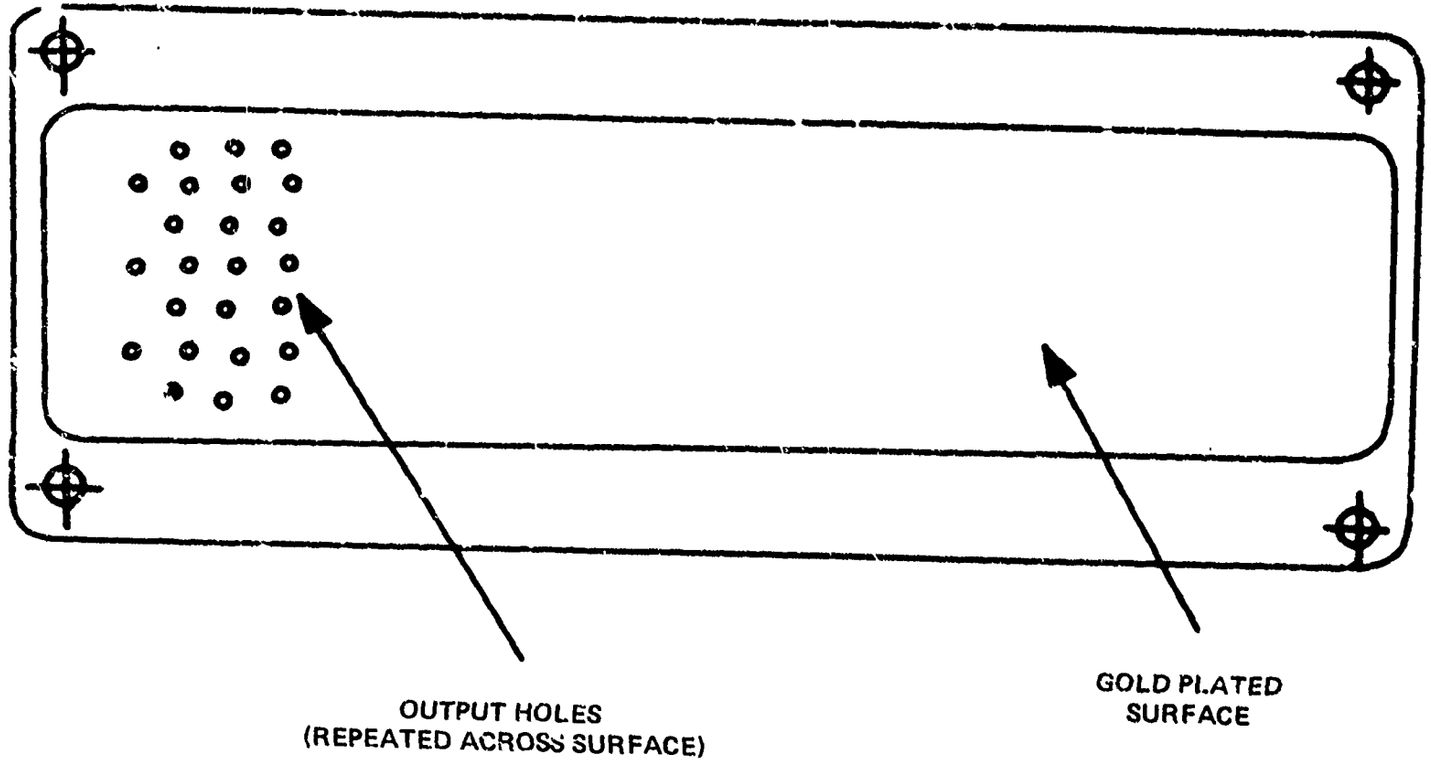

FIGURE 18. DIAGRAM OF OUTPUT MIRROR

from the throat. NaCl windows are mounted at the sides of the cavity, approximately 2 inches behind each mirror. Each window serves as a vacuum seal, and the beam is extracted through one of these windows. Pressure may be monitored through a port in the top of the cavity. Various dry gases such as A or N_2 may be used to purge the windows to protect them from moisture or harmful gases in the flow.

3.4 The Assembled Special Configuration Laser

This section presents photographs of the SCL, taken in partially and completely assembled views. Figures 19 and 20 view the SCL from opposite sides and ends. Starting from the upstream end, the center electrode and a special water flow connector of the plasma generator are shown. Next the generator with its field winding and housing are shown, supported on the generator base. This is followed by the plenum, nozzle, cavity, and end transition sections. On each side of the cavity are the mirrors and NaCl windows. The output window is the largest. The other window is suitable for gain measurements with the mirrors removed and for alignment purposes when the mirrors are used.

Figure 21 views the SCL from above and opposite the output side of the cavity. The large vacuum tank may be partially seen on the right. Vacuum pumps are at the top of the picture. Several of the He and CO_2 supply bottles are seen at the bottom. Most of the other components of the SCL may also be seen. Figure 22 is the same, except viewed from the output side of the cavity.

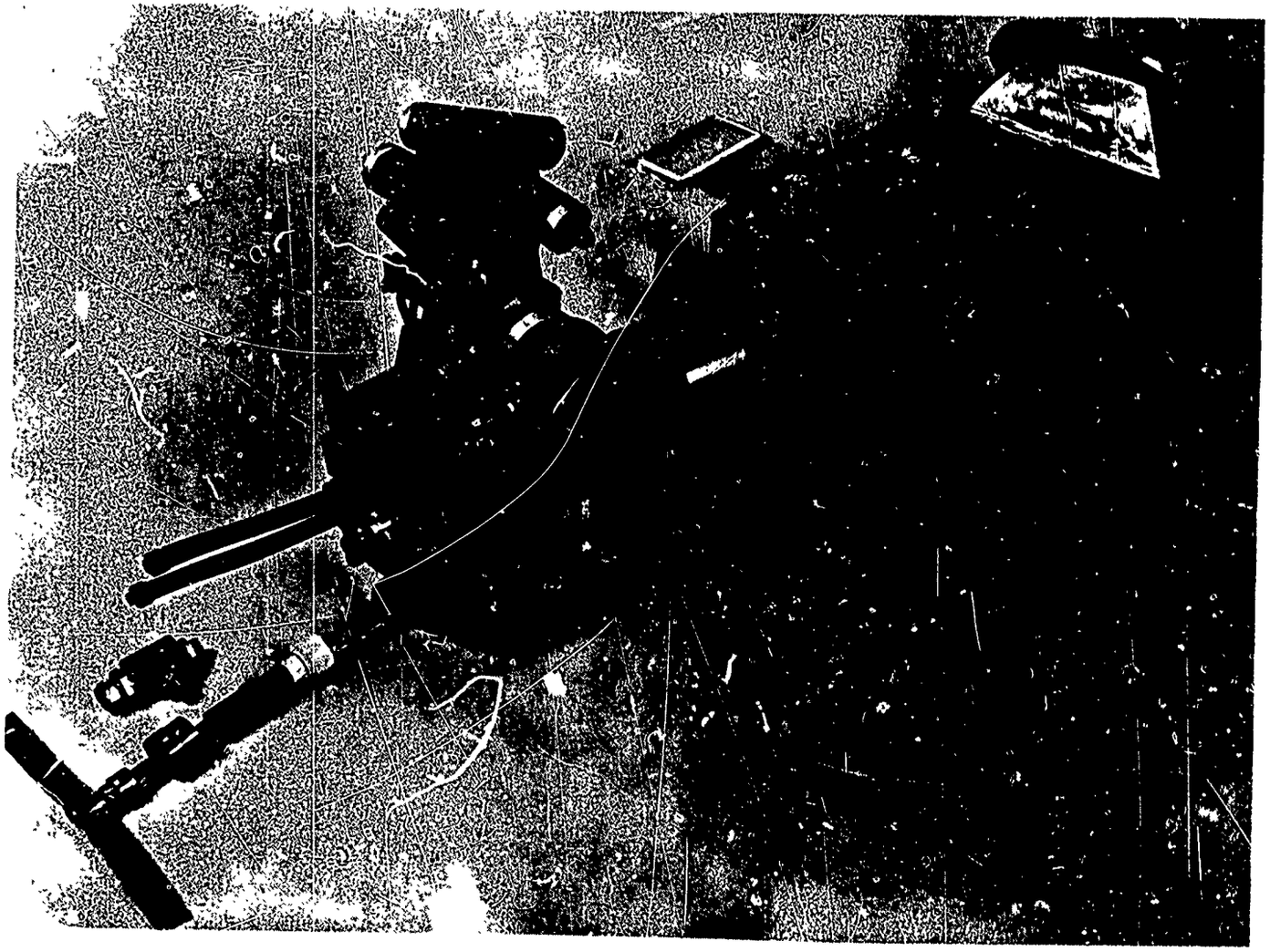

FIGURE 19. PHOTOGRAPH OF SPECIAL CONFIGURATION LASER, EXPLODED, VIEW 1

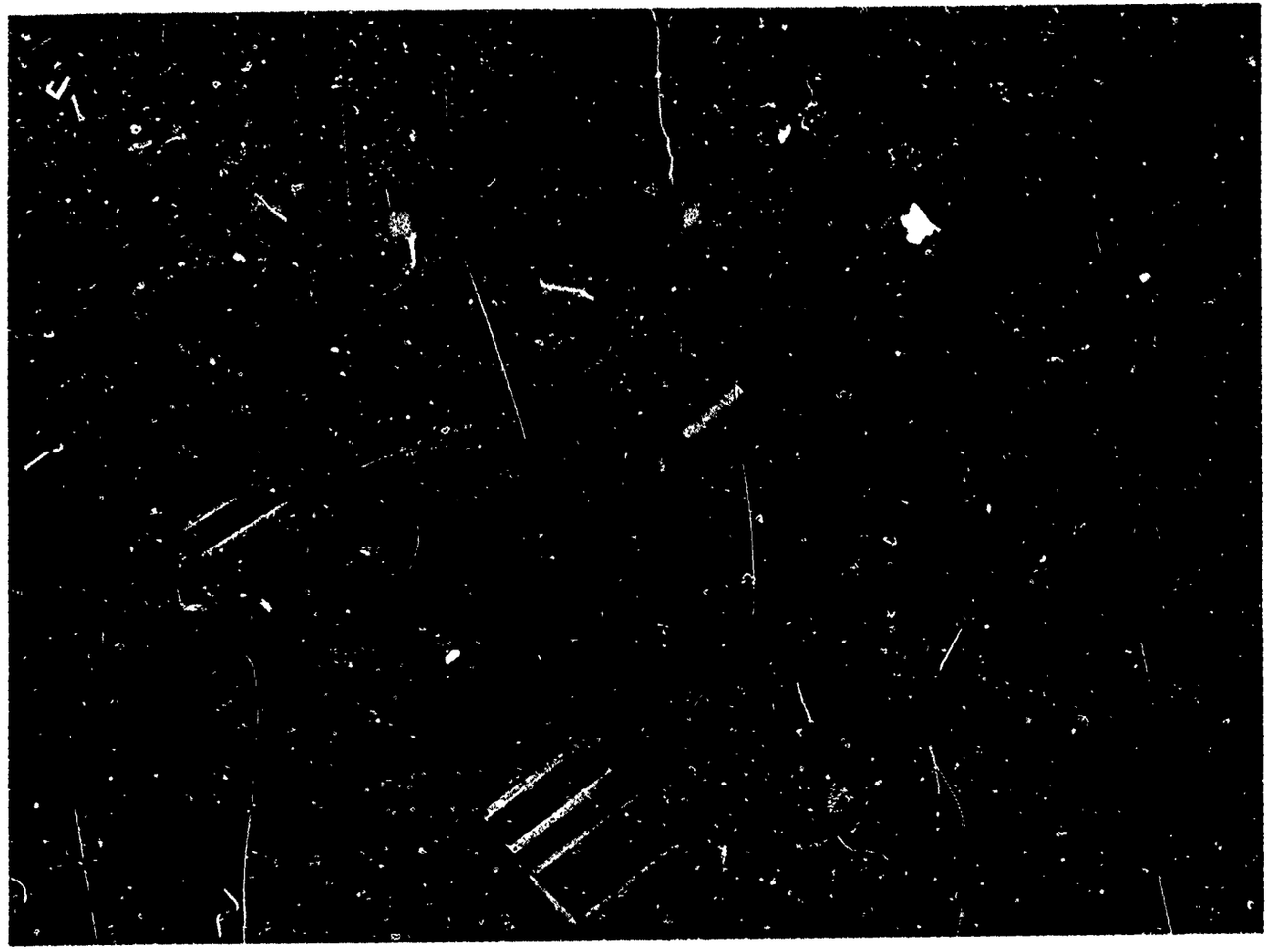

FIGURE 20. PHOTOGRAPH OF SPECIAL CONFIGURATION LASER, EXPLODED, VIEW 2

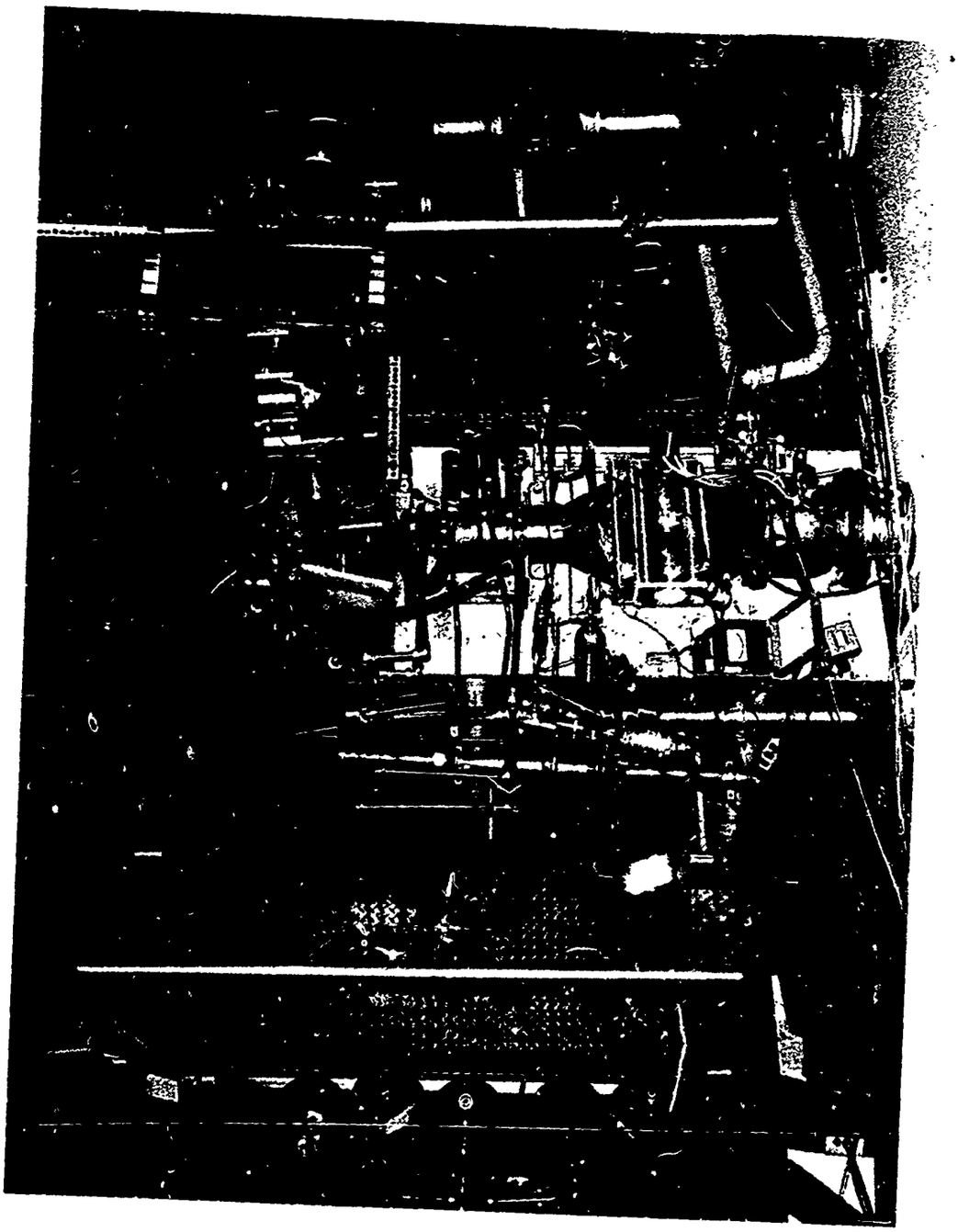

FIGURE 21. PHOTOGRAPH OF SPECIAL CONFIGURATION LASER, VIEW 3

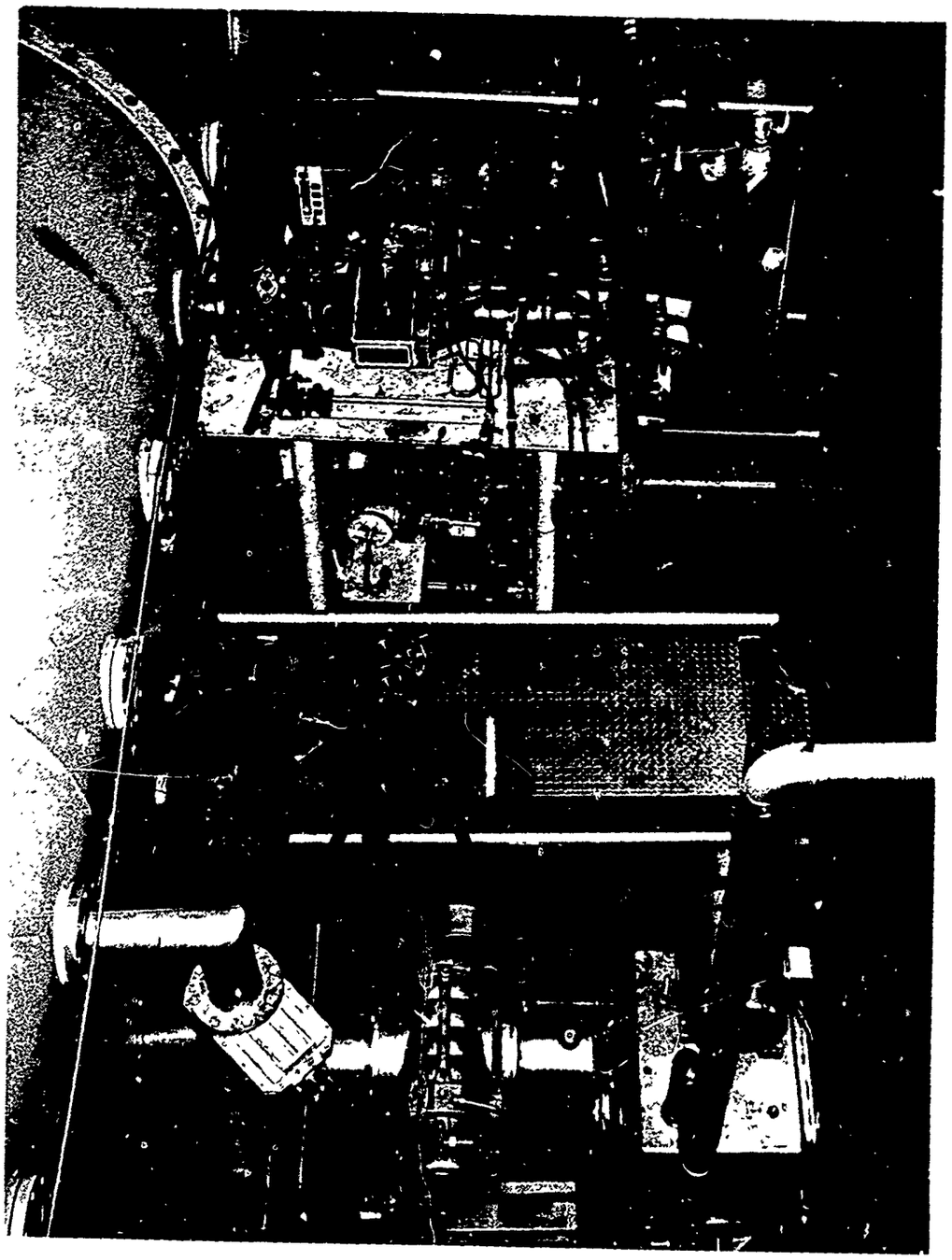

FIGURE 22. PHOTOGRAPH OF SPECIAL CONFIGURATION LASER, VIEW 4

CHAPTER 4

INSTRUMENTATION AND CALIBRATION

This chapter discusses the various parameters that are measured when the laser is operated. The associated equipment is also covered. Calibration of the various instruments and reduction of data is discussed. In general, the most important parameters are input and output powers, gas flow rates, and temperatures of the gases. Each of these are considered in this section.

4.1 Measurement of Gas Flow Rates

Pressure transducers in the gas lines (Figure 9) and the SCL itself monitor the component gases, both individually and after mixing. For the most part these are slide wire transducers, Model 842-A, and manufactured by Sparton Southwest. In operation the N_2 pressure to the arc and the plenum is recorded as well as the CO_2 and He pressures in their respective lines. The plenum pressure is monitored immediately upstream from the nozzle. The N_2 back pressure on the H_2O reservoir is also measured, since it controls the flow rate of the water.

A 5 volt dc signal is applied across each slide wire transducer. Acting like a potentiometer, the transducers emit a 0 to 5 volt signal, corresponding to the percentage of the maximum rated pressure that is applied to the transducer. This signal is amplified

by a Preston 8300 or 8300 XWB amplifier and fed into a Brush Mark 200 recorder, Model RF 1783-40, or a Sanborn Model 154-100B recorder.

Cavity pressures may be monitored by an MKS Baratron Pressure Meter, Type 90M-XRP. Numerous diaphragm gauges throughout the supply lines give visual indication of gas pressures, especially the dome regulating pressures.

4.1.1 Calibration Procedures

N_2, CO_2, and He gases are injected into the system through sonic orifices. The size of the orifice, the upstream pressure P_o and temperature T_o, and the gas properties determine the flow rate of each gas through its orifice. Orifice sizes were obtained theoretically for the range of flow rates desired, and later checked experimentally.

For a given set of upstream conditions of a gas, the flow rate through an orifice will increase as the absolute pressure ratio P/P_o decreases, until the velocity of the gas in the throat reaches that of sound in the gas. At this point the Mach number is unity and the orifice has become sonic. The pressure ratio then becomes

$$\frac{P}{P_o} = \frac{P^*}{P_o} = r_c$$

where r_c is the critical pressure ratio and where conditions at the throat are denoted by an asterisk (*). It can be shown [38] that

$$r_c = \left(\frac{2}{k+1}\right)^{\frac{k}{k-1}}$$

where k is the ratio of constant pressure to constant volume specific heats. Depending upon gases and temperatures, r_c is usually between 0.5 and 0.6. To insure that the orifice is sonic, P_o is kept at least twice as large as P^*.

If the ratio of the cross-sectional areas S_o/S^* is 25 or more, then the mass flow rate is given [38] by

$$\dot{m} = C_v \, S^* \, P_o \left[\frac{k g_c M}{T_o \, R} \left(\frac{2}{k+1} \right)^{\frac{k+1}{k-1}} \right]^{1/2} .$$

Here C_v is a coefficient of velocity and is near unity. M is the molecular weight, g_c is a gravitational constant numerically equal to the acceleration of gravity, and R is the gas constant per mole.

This equation was used to determine orifice sizes S* for each gas, given the required flow rates and upstream pressures. With the orifices in place, more accurate plots of P_o versus $\dot{m}$ were obtained experimentally. With the pumps shut off, gases were injected through the orifices and into the vacuum tank for a measured length of time. A knowledge of the tank volume and tank pressure before and after the gas flow allowed the total mass flow rates to be determined.

In equation form:

$$\dot{m} = M \frac{V}{RT} \frac{\Delta P}{\Delta t}$$

were V is the tank volume. (This equation is derived by differentiating the ideal gas law with respect to time, t.) Then a graph of $\dot{m}$ as a function of the upstream pressure P_o may be plotted. During an actual laser run the transducer pressure readings of P_o are recorded and the mass flow rates are subsequently determined from the experimentally determined graph of $\dot{m}$ versus P_o.

The tank volume was again measured by connecting a gas cylinder of known volume to the tank and allowing some gas to flow into the tank. If the cylinder and tank pressures are recorded before and after the gas flow, the number of moles, n = m/M, lost by the cylinder

being measured in the vacuum tank, the water is caught and measured while still a liquid.

4.1.2 Calculation of Mass and Molar Fractions

It is also convenient to know the percentage of each gas in the flow. Gas percentages or fractions may be given in either of two ways: mass fractions or molar fractions.

By definition, the mass fraction is given by

$$f_{m_i} = \frac{m_i}{\sum_n m_n} = \frac{m_i}{m_t} \quad .$$

Here m_i is the mass of the ith gas, and m_t is the total mass of all the gases. In this case mass flow rates may be substituted for the masses, and the mass fraction easily determined.

In addition to mass fractions, gas components are often given in terms of molar fractions. By definition, the molar fraction is given by

$$f_i = \frac{N_i}{\sum_n N_n} \quad .$$

Here N_i is the number of moles, m_i/M_i, M_i is the molecular weight of the ith gas, and the index n is summed over all constituent gases. To obtain molar fractions from mass fractions:

$$f_i = \frac{N_i}{\sum_n N_n} = \frac{\frac{m_i}{M_i}}{\sum_n \left(\frac{m_n}{M_n}\right)} = \frac{\frac{m_i}{m_t}}{M_i \sum_n \left(\frac{\frac{m_n}{m_t}}{M_n}\right)}$$

or

$$f_i = \frac{f_{m_i}}{M_i \sum_n \frac{f_{m_n}}{M_n}} .$$

Conversely, to obtain mass fractions from molar fractions, solve the last equation for f_{m_i}.

$$f_{m_i} = f_i M_i \left[\sum_n \frac{f_{m_n}}{M_n} \right]$$

$$= f_i M_i \left[\frac{1}{m_t} \sum_n \frac{m_n}{M_n} \right] = f_i M_i \left[\frac{1}{m_t} \sum_n N_n \right]$$

$$= f_i M_i \left[\frac{1}{\sum_n \frac{\frac{m_n}{M_n} \times M_n}{\sum_n N_n}} \right]$$

or

$$f_{m_i} = f_i M_i \left[\frac{1}{\sum_n f_n M_n} \right] .$$

Therefore, given the mass flow rates and molecular weights, either mass or molar fractions may be determined. Gas percentages may then be compared to flow percentages given in the literature, regardless of which form is used.

4.2 Plenum Temperatures T_o and T_{wall}

An important parameter in gas-dynamic studies is the gas temperature T_o, measured just prior to expansion through the nozzle. In the SCL there is a port for this purpose located on top of the plenum hardware, immediately upstream from the center of the nozzle. Standard platinum versus platinum 10 percent rhodium thermocouples are

used to monitor the gas temperature. The output signal of a few millivolts in magnitude is amplified by a Preston 8300 amplifier and then displayed on the Brush recorder. Conversion charts [39] that relate output voltages to temperatures are later used to determine the temperature of the gas flow.

The gas temperatures depend upon how much power is given to the plasma arc and also the gas flow rate. Recorded temperatures ranged from 1300° to 1700°K for the input powers and flow rates that were used.

One problem in experimentation was overheating of the hardware after a run. Conduction from the arc soon heated the plenum, as did the hot gas in the plenum. This heat was conducted downstream into the nozzle and cavity. (The problem will be further discussed in section 4.5.) It was found necessary to monitor the temperature of the plenum hardware and allow time between runs for the hardware to cool. Designated as T_{wall}, this temperature was measured by a Temco Portable Pyrometer and Millivoltmeter, Model PM-1K17. Essentially this is a thermocouple in thermal contact with the top of the expansion or transition section of the plenum.

Readings were taken from the millivoltmeter before and after each run. At various times the effect of purposefully overheating the hardware was studied; the results of these tests will be discussed in Chapter 6.

4.3 Input Power

Power delivered to the arc is usually on the order of 10^6 watts. Typical current and voltage levels are 2600 amperes at 390 volts.

However, the input power has been varied from 0.6 to 1.2 megawatts. Although each of the six generators is capable of producing this power, it is easier to obtain desired power levels over a wide range of gas flows with two generators in series driving one arc.

Again referring to Figure 5, the arc voltage is measured by a shunt across the arc and one contactor. The current is measured between the ground side of the arc and the field winding by using a water-cooled high current shunt in series. The voltage drop across this element determines the arc current. Voltage and current levels are displayed on a Sanborn Model 850 strip recorder.

From the differential form of the heat equation (power $= \dot{m}c\Delta T$), an estimated 20 to 25 percent of the input energy is coupled into the gas.

4.4 Output Power

The 10.6 micron laser output was recorded in three ways. For a quantitative power measurement, a thermopile detector system was used. To determine which section of the cavity is lasing, i.e., at what distance from the throat lasing occurs, another method must be used. This type of information was obtained from patterns burned into thermofax paper or polyurethane foam packing material.

4.4.1 Thermopile Detector System

Power output measurements (in watts) were obtained by using a Coherent Radiation Laboratories Model 203 Power Meter. Radiation was gathered by a 6-inch concave mirror with a 24-inch focal length. The beam was then focused into the array of thermocouples in the detector. Instead of using the manufacturer's amplifier and meter, a Preston 8300

amplifier fed the signal into the strip recorder.

4.4.2 Laser Burn Patterns

It was desired to know at what positions in the cavity that lasing occurs. Depending upon the gas flow mixtures and the effects of additives, the output beam may vary in several ways as the distance from the throat varies. For some gas mixtures most of the lasing occurs on the upstream side of the mirror, with very little radiation emitted further downstream. In other cases, the beam may be fairly uniform across the mirror face. To observe these effects, patterns were burned into several materials by placing them in front of the output mirror. Two materials were found to be most useful for beam detection.

For the small output power densities obtained in Mode I, heat sensitive thermofax paper, of the type used in some strip recorders, was found to be quite useful. This material can withstand an estimated 10 watts per square inch for several seconds before being completely penetrated.

For higher power levels, patterns were burned into polyurethane packing material, a white foam substance similar in texture to a cross between foam rubber and styrofoam. It is tough, slightly resilent, and nearly incombustible for power densities on the order of 50 watts per square inch or less.

The depth of the burn or the volume of the cavity formed is proportional to the energy deposited. (There is a threshold power density which must be exceeded before the polyurethane is damaged.) The varying depths and volume of each burn have been measured. Plaster of Paris castings were also made for future reference.

Additional burn patterns were produced with a conventional 100 watt laser, in order to compare energy and power levels with burn depths and volumes. Figure 23 plots the total laser energy as a function of the volume of the burn cavities. The threshold for damage of the polyurethane may be noted by the positive y-intercept. Although not shown, it is also possible to plot the energy density as a function of the depth of the burn. The result is a graph very similar to the one in Figure 23.

Quite a bit of experimental data was taken in pairs, the thermopile detector used in one run and the polyurethane in the other, all other parameters equal. In this way it is possible to correlate the size and shape of a burn pattern with a power reading. However, in operation the output power increases slightly for 4 or 5 seconds and then drops because of heating of the hardware. Power readings given in this report are the maximum obtained during the run. It is not possible to correlate this maximum power with the burn volumes. Instead an effective or average power must be compared to the corresponding burn volume. Although not shown, this can be obtained by integrating the area under the curve of the thermopile output signal on the strip recorder.

4.5 Problems Encountered

With virtually any new or different piece of equipment, the early models tend to possess inherent design or construction defects and inconveniences. This is especially true with state of the art experimental equipment whose optimized theoretical design may be worth less than last week's newspaper by tomorrow. The SCL is no

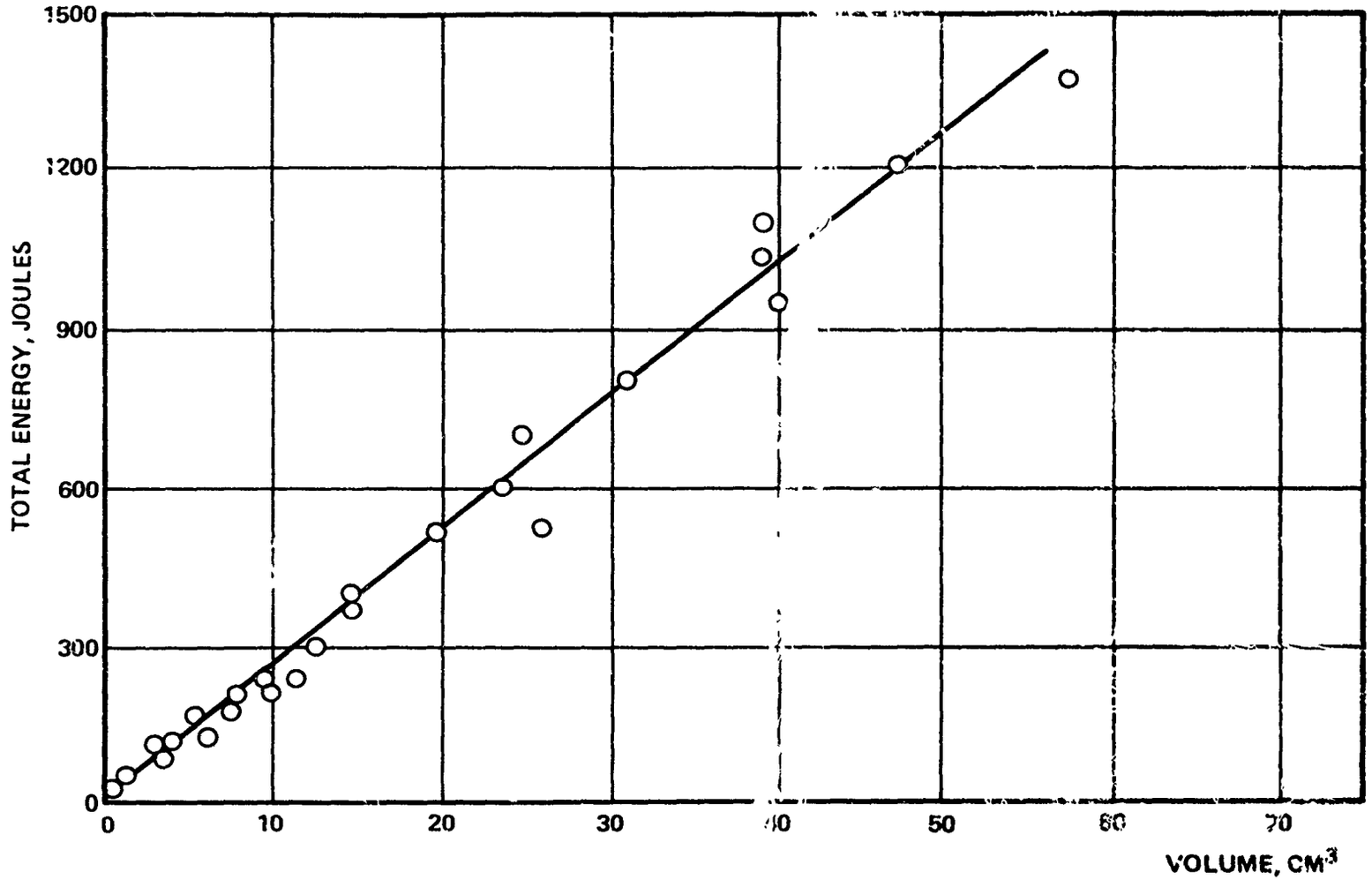

FIGURE 23. GRAPH OF OUTPUT ENERGY VERSUS BURN VOLUME

exception. Although it did produce valid, worthwhile results, it does have some shortcomings.

Two major disadvantages kept the SCL from operating as well as desired. First, the hardware was designed to be used with six arc heaters. Only one arc was made available by the Plasma Facility. So optimum pressures, temperatures, and gas flow rates could not be reached, especially for the GDL or Mode I experiments. Second, the plenum and other hardware overheated after a few seconds and must then be allowed to cool before it was operated again.

Since these difficulties did exist, a new system was designed and is now being assembled. The new system will correct these and other minor problems. This has allowed only a minimum amount of time to be spent on the SCL, as work had to be stopped prematurely to make space and equipment available to its successor. As a consequence, much less information was obtained than was desired.

The remainder of this report deals with the results obtained during the period the SCL was available for experimentation.

CHAPTER 5

EXPERIMENTAL RESULTS OF GAS-DYNAMIC LASER (MODE I) OPERATION

As mentioned earlier, desired plenum pressures and temperatures could not be reached with the single arc system. Typically the pressure P_o should be 15 to 20 atmospheres at a temperature of 1400° to 2000°K. The SCL as described in Chapter 3 could obtain 4 atmospheres of stagnation pressure with temperatures up to 1700°K but not at the same time. Typically P_o was near 2 or 3 atmospheres and T_o was near 1400°K. A limited amount of data was taken in the gas-dynamic mode, since most of the available time was spent operating in the supersonic mixing mode. Several conclusions may be drawn, however, and are presented below.

5.1 Maximum Power Versus N_2 Flow Rate

Figure 24 is a graph of the output power as a function of the nitrogen flow rate at constant CO_2 and H_2O flow rates. The output increases up to a point, at which more N_2 slightly decreases the beam intensity. Maximum power obtained was only 15 watts and the ordinate is normalized to this value. Since N_2 alone is heated in the arc, there are lower limits at which the N_2 flow rate may be set and still keep a steady plasma arc. For this reason no data is shown for lower N_2 gas flows.

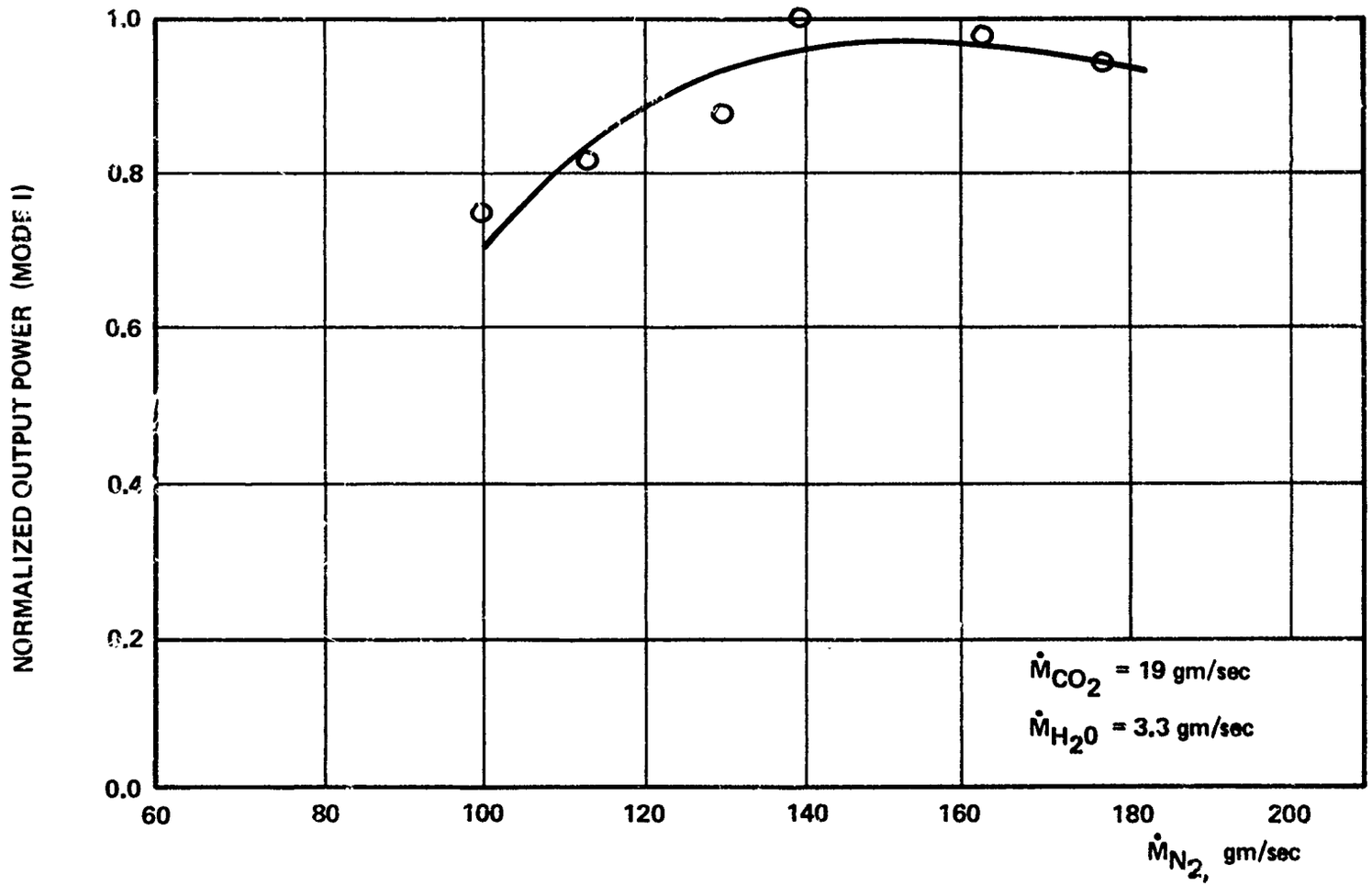

FIGURE 24. GRAPH OF OUTPUT POWER VERSUS N_2 FLOW RATE (MODE I)

5.2 Power Versus H_2O Flow Rate

For this data patterns were burned into thermofax paper (Figure 25). N_2 and CO_2 flow rates were held constant as indicated and the molar fraction of H_2O was varied from 1.8 to 5.8 percent. No burn was obtained for the lowest percentage of water. The other data is shown in the figure. The heavy lines on each side indicate the positions of the first and last rows of output coupling holes. These are separated by a distance of about 5.13 inches.

As seen in the photograph, the cross-sectional area of the beam increases with the output power. The peak intensity occurs slightly upstream of the center of the optical cavity. No power was extracted from either end of the cavity. Maximum output was with 3 percent water, with additional water decreasing the beam intensity.

5.3 Summary of Mode I Operation

From the two previous sections and other data not presented here, several observations may be made concerning the SCL operating in the gas-dynamic mode with marginal plenum conditions. Mixture ratios affect the output beam quite strongly, especially the ratio of water vapor. No output was obtained without using water, but maximum intensity occurred with only 3 percent water. N_2 and CO_2 composed 86- and 11-percent respectively, of the gas flow. Operating under the marginal conditions described above, maximum power was only 15 watts. (A few earlier attempts were also made using helium as an additive, but no output power was obtained.)

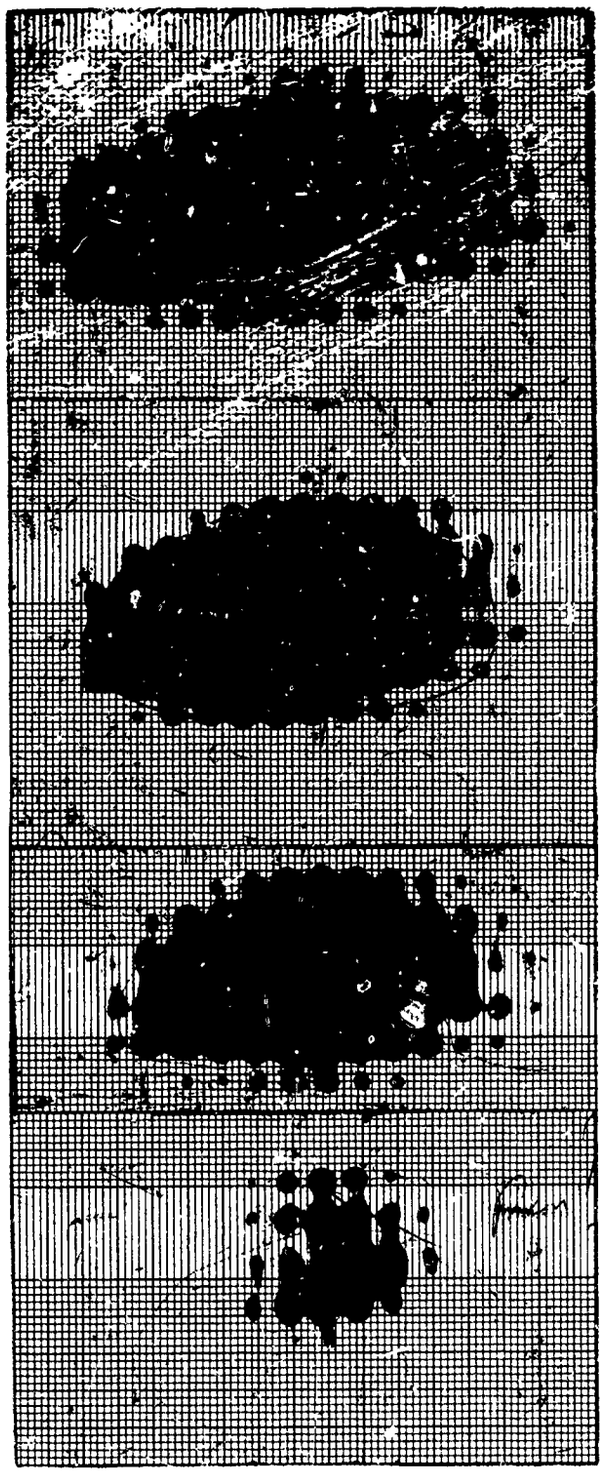

$\dot{M}_{H_2O}$ (F_{H_2O})

2.2 gm/sec (3%)

3.3 gm/sec (4.4%)

4.0 gm/sec (5.3%)

4.4 gm/sec (5.8%)

$\dot{M}_{N_2}$ = 100 gm/sec, $\dot{M}_{CO_2}$ = 19 gm/sec

FIGURE 25. PHOTOGRAPH OF BURN PATTERNS, H_2O VARIATION (MODE I)

CHAPTER 6

EXPERIMENTAL RESULTS OF SUPERSONIC MIXING (MODE II) OPERATION

In this mode CO_2 is mixed into the supersonic flow immediately downstream of the three nozzle throats. With particular mass flow rates, powers on the order of 275 watts were obtained. This chapter presents data from Mode II. In particular, variation of beam power due to the individual gas flow rates, as well as other factors, is presented.

6.1 Effects Due to T_{wall}

As mentioned earlier, the hardware overheats after several seconds of operation. In doing so, the output power drops as in Figure 26. T_{wall} is measured as described in Chapter 3, and is a function of the temperature of the plenum outer wall. The output power has been normalized to the highest value obtained for this set of data, which is near 150 watts. In addition, it was found that the spatial pattern produced by burning the polyurethane was also affected. As T_o rises, the beam shifts more and more toward the upstream end of the cavity. At high enough temperatures all of the beam emerges from the upstream 40 percent of the cavity, with this portion greatly reduced in intensity.

Several factors may be contributing to this effect, which also takes place in other modes of operation. The alignment of the

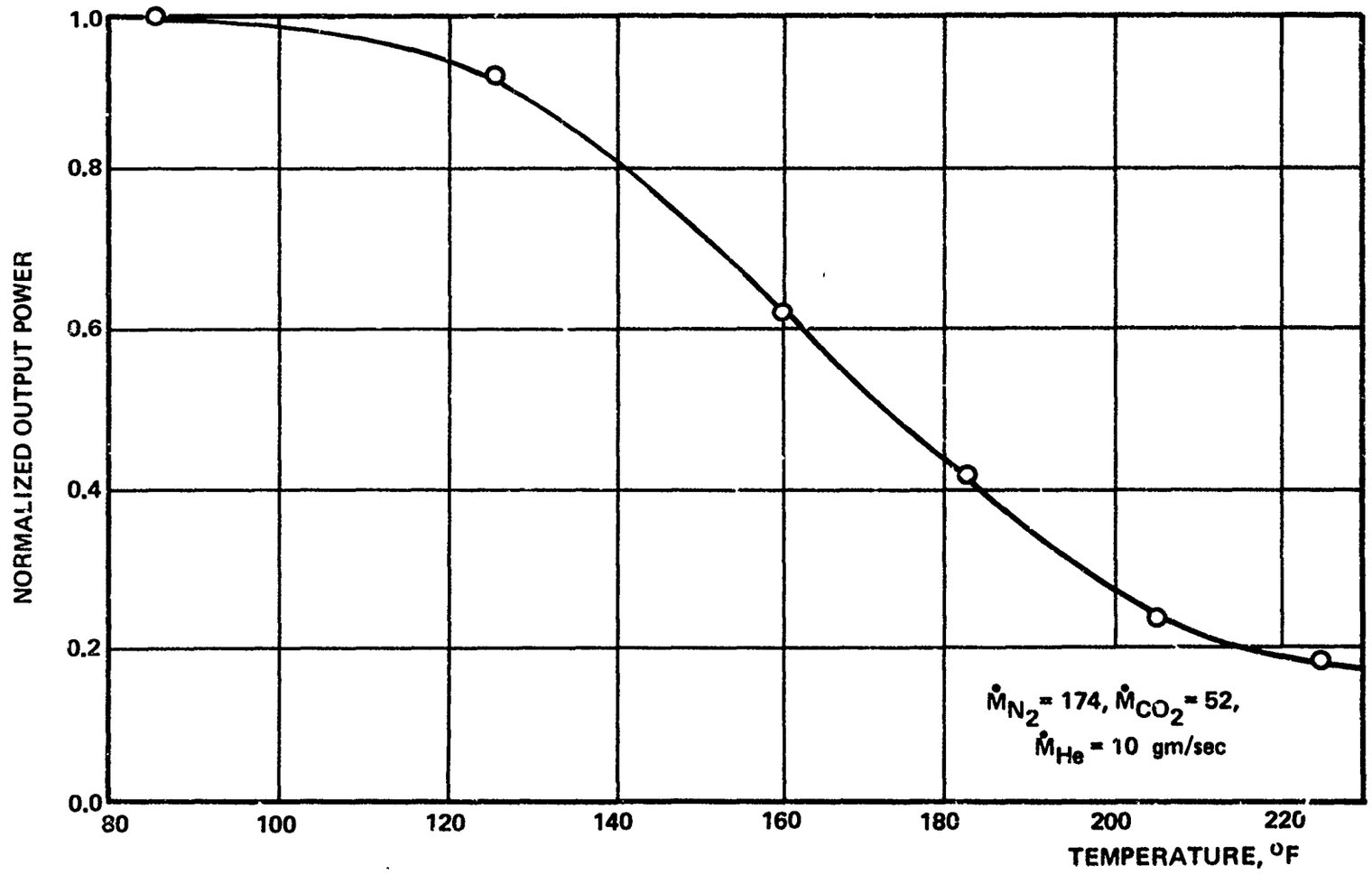

FIGURE 26. GRAPH OF OUTPUT POWER VERSUS T_{wall} (MODE II)

mirrors may be changing as the cavity heats, or the hot walls may be affecting the rate at which lower levels are depopulated. In any case, the problem was eliminated by separating each 5-second run by a period of two or more hours. During this time the hardware was allowed to cool to near room temperature.

6.2 Power Variation Due to the N_2 Flow Rate

Figure 27 is a graph of normalized output power as a function of the N_2 flow rate. In this and succeeding data, the power output has been normalized to the maximum value obtained with supersonic mixing. Two curves are shown, corresponding to two different CO_2 mass flow rates. In general, output increases until a point is reached where further addition of N_2 has little or no effect. If extended to lower N_2 flow levels, the curves would drop rather sharply.

Figure 28 is a spatial representation of the beam pattern obtained by burning polyurethane. The horizontal axis plots the distance from the first row of output coupling holes in the mirror. The vertical axis represents the depth of the burn and is a function of the energy deposited by the beam. This coordinate then gives a representation of the intensity of the beam. The axis out of the page represents different N_2 flow rates.

Corresponding to the previous figure, not much change in power is observed while varying the N_2 flow. The most important feature is the dominant peak in the curve near the upstream end of the cavity or at low values of z. Note that no helium was used in this set of data. This feature will be further discussed in section 6.4.

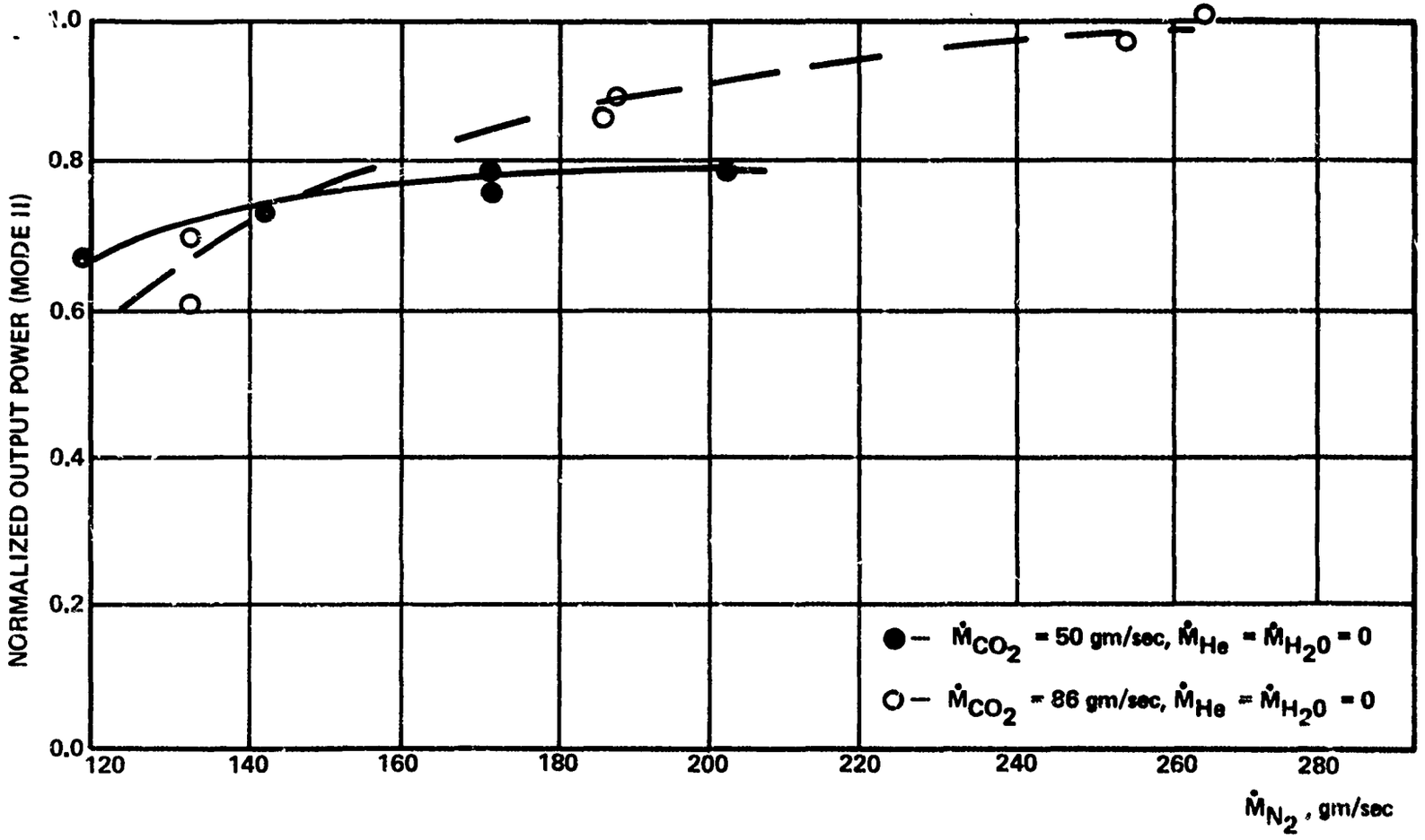

FIGURE 27. GRAPH OF OUTPUT POWER VERSUS N_2 FLOW RATE (MODE II)

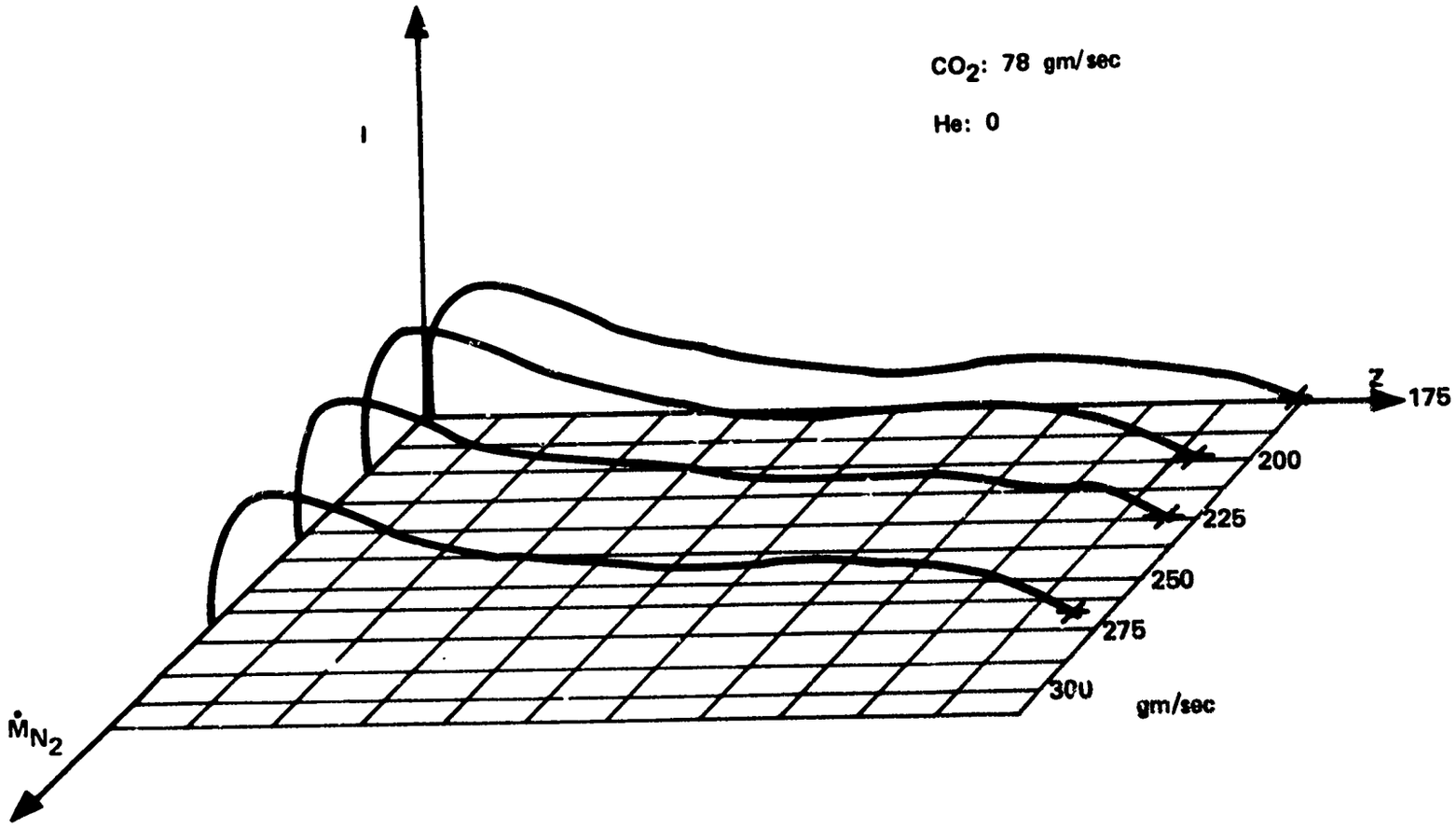

FIGURE 28. SPATIAL BURN PATTERNS WITH N_2 VARIATION (MODE II)

6.3 Power Variation Due to the CO_2 Flow Rate

Figure 29 is a graph of normalized output power as a function of the CO_2 flow rate. Two curves are given, one with and one without helium. In addition the mass flow rates of N_2 are slightly different for the two curves. Over the regions covered, the output power varies almost linearly with the CO_2 flow rate. Note also the run with helium produces lower power.

Figures 30 and 31 are spatial representations of burn patterns, taken while varying the CO_2 flow. The N_2 flow rates are not the same for the two figures but the important difference is that Figure 30 was obtained with helium, while Figure 31 was obtained without helium. Note that with helium there is not too large a peak at low values of Z, while there is a peak in Figure 31, at least for higher CO_2 flows. These peaks tend to occur in runs not containing helium and at higher CO_2 flow rates.

6.4 Power Variation Due to the He Flow Rate

Figure 32 is a graph of the normalized output power as a function of the helium flow rate. Note that the power decreases for increasing gas flow, with a sharper drop at the higher He flow rate. Maximum power occurs when no helium is used.

Then compare this information with that given in Figure 33. Note here that increased amounts of helium decreases the initial peak and tends to flatten the burn pattern. The total burn volume is smaller but is deeper for higher values of Z than for the data with no helium. (Although the lower He flow rates produce a longer burn pattern, this may be due to edge effects and the mirror configuration.)

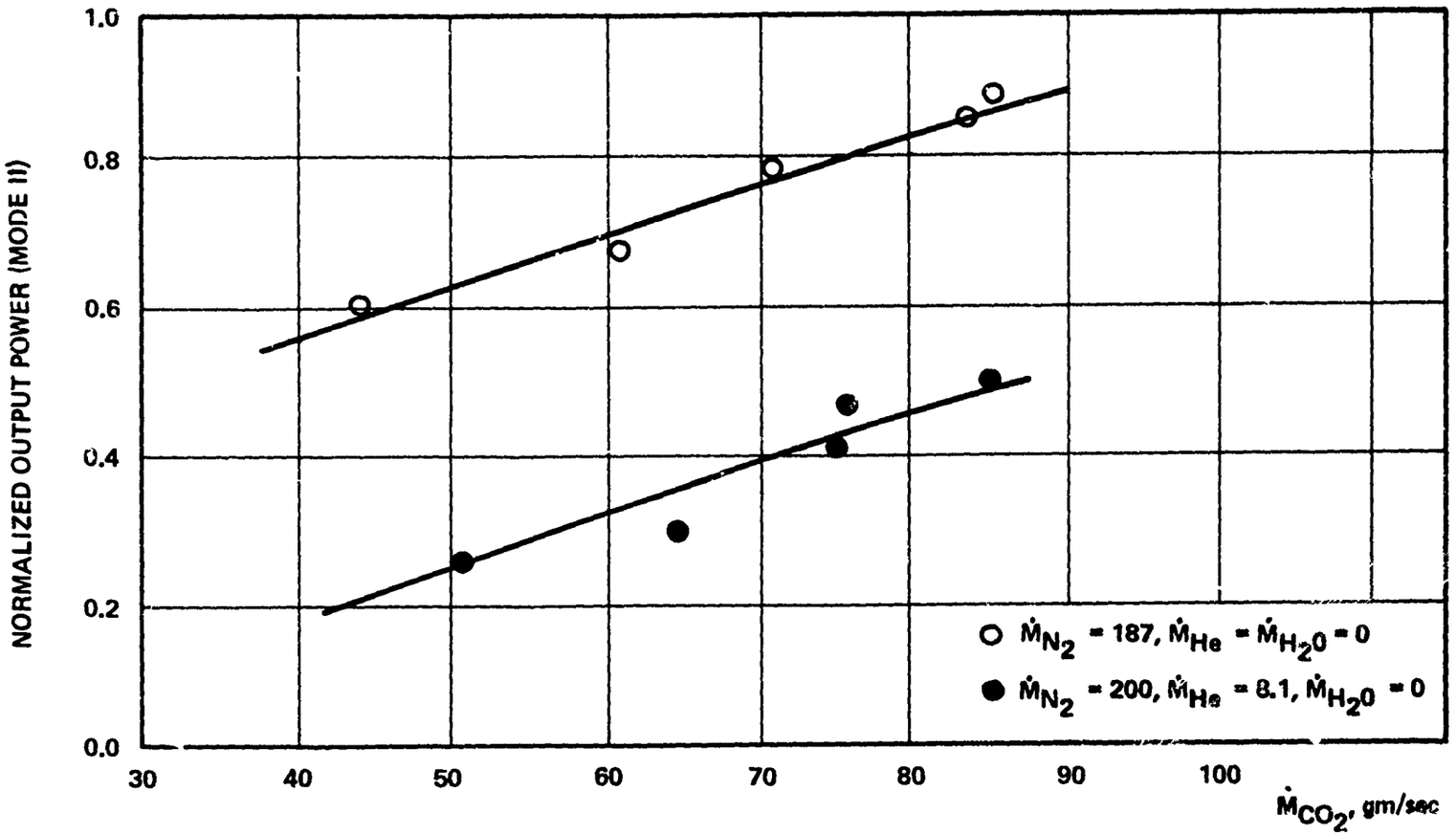

FIGURE 29. GRAPH OF OUTPUT POWER VERSUS CO_2 FLOW RATE (MODE II)

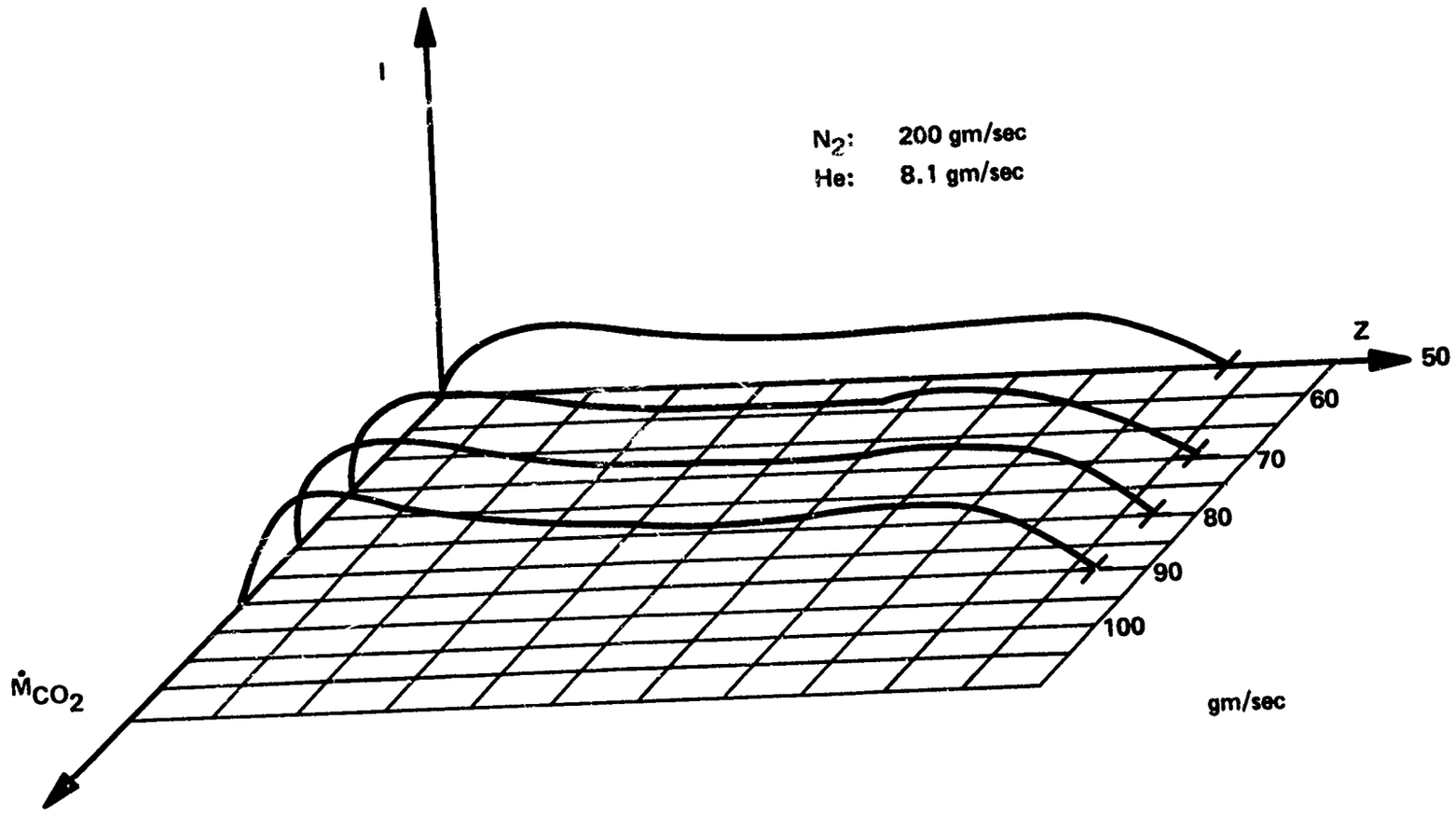

FIGURE 30. SPATIAL BURN PATTERNS WITH CO_2 VARIATION (MODE II) A

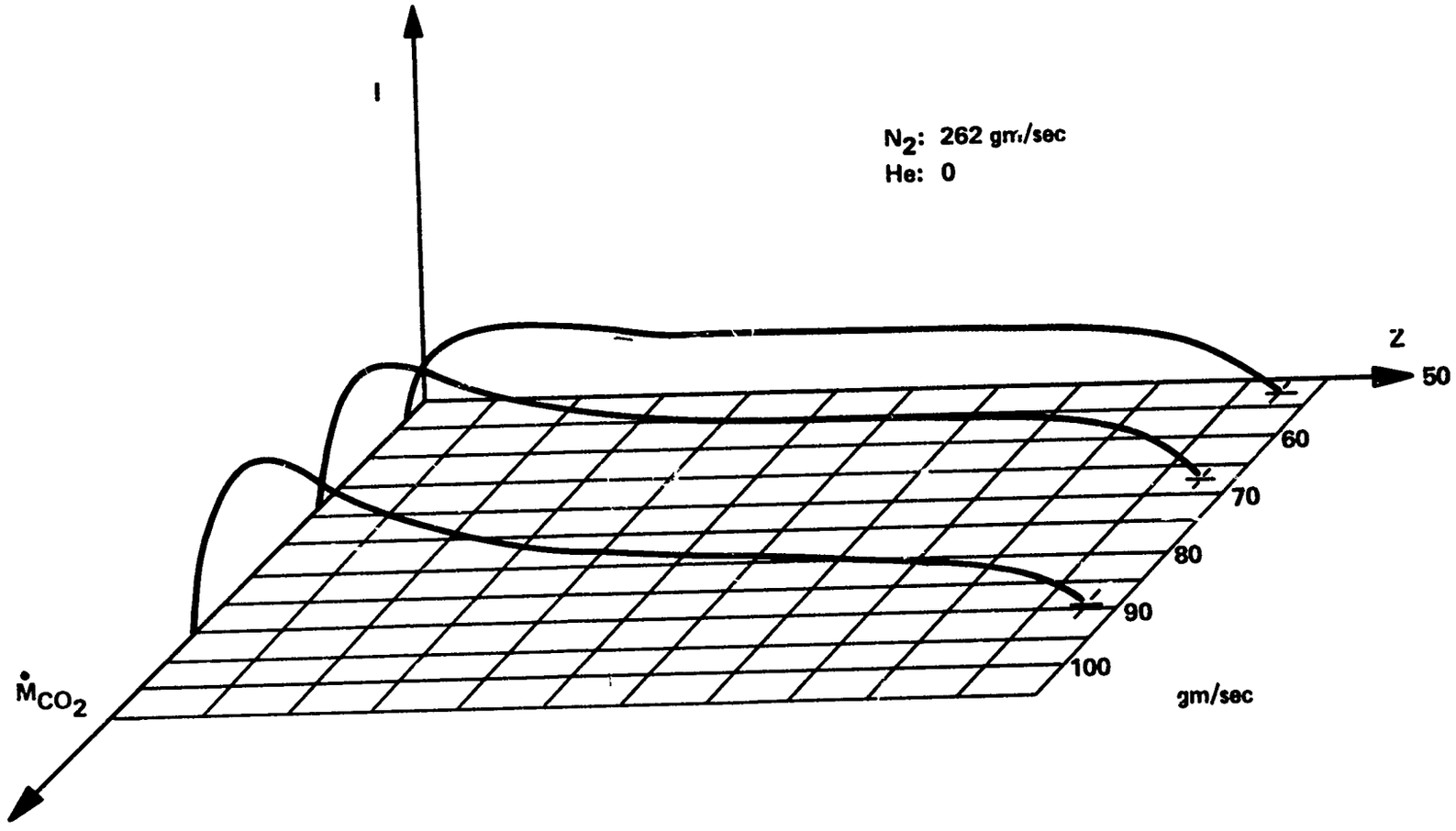

FIGURE 31. SPATIAL BURN PATTERNS WITH CO_2 VARIATION (MODE II) B

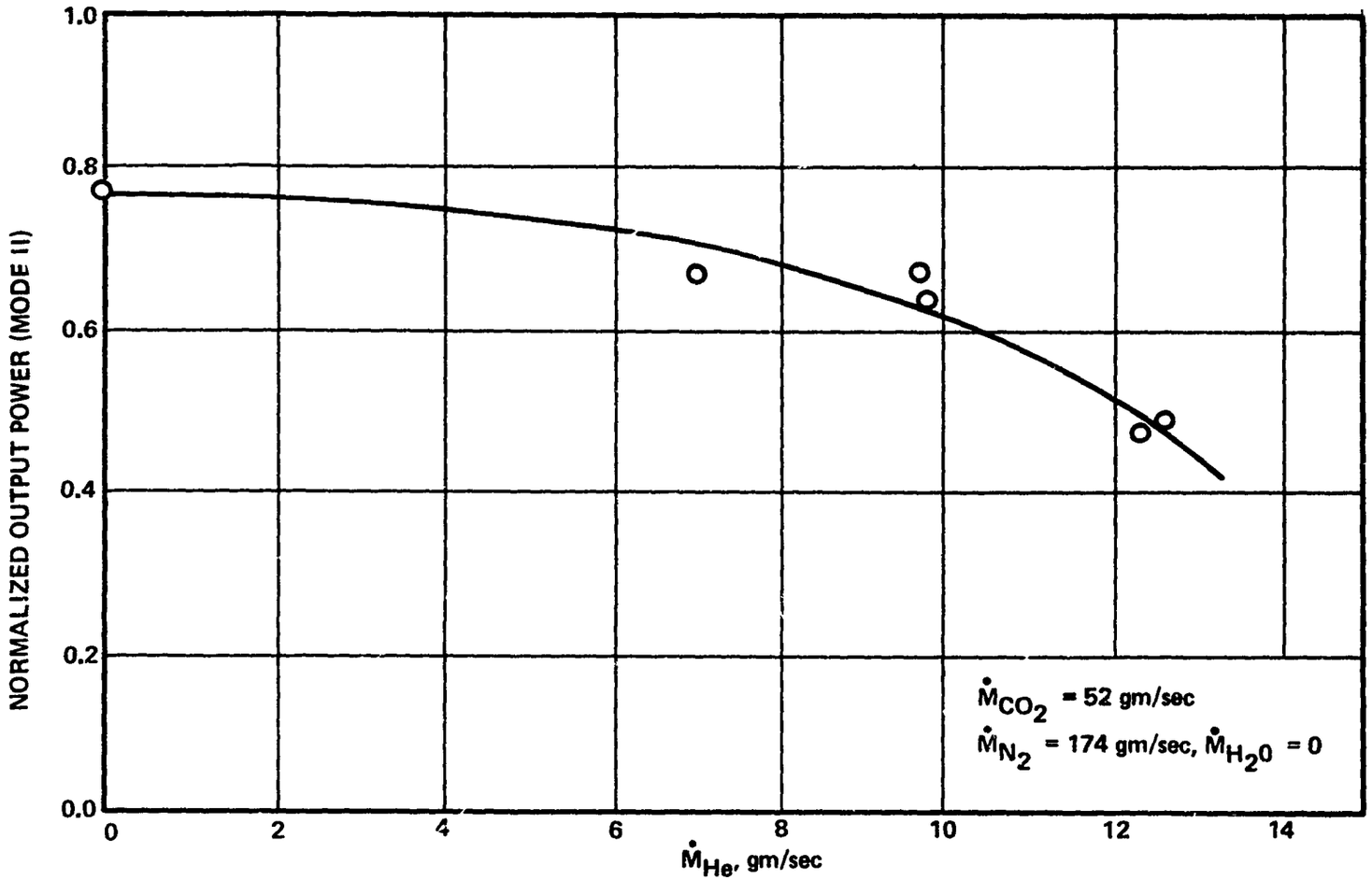

FIGURE 32. GRAPH OF OUTPUT POWER VERSUS He FLOW RATE (MODE II)

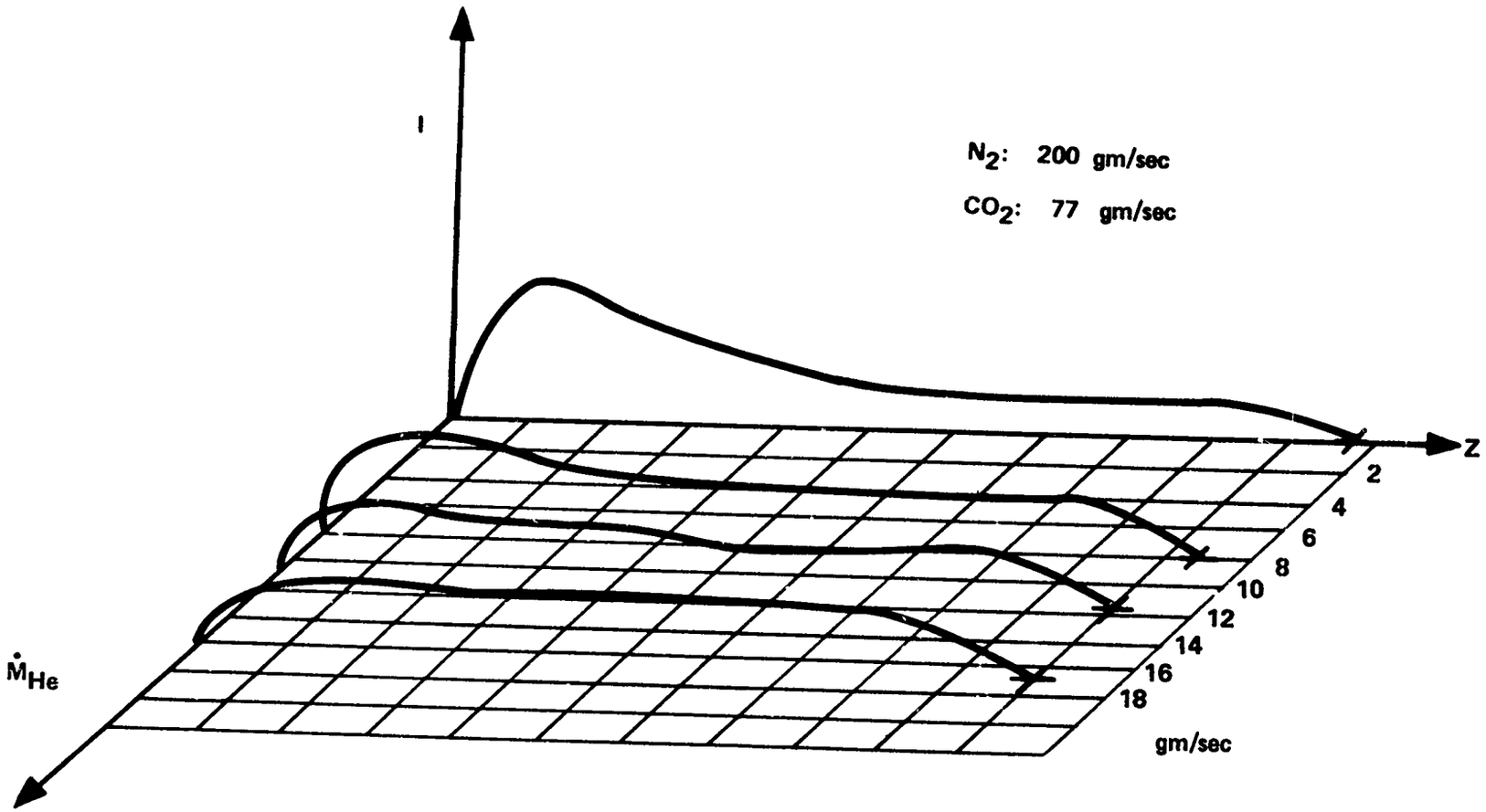

FIGURE 33. SPATIAL BURN PATTERNS WITH He VARIATION (MODE II)

From these figures and those in the two previous sections, it may be concluded that helium does not increase total power from the SCL in Mode II operation. However, it does tend to produce a smoother, more uniform beam over the cavity length. It is quite likely that with a longer cavity the lasing conditions might remain the same for some distance. In this case the addition of helium might be advantageous.

6.5 Power Variation Due to the H_2O Flow Rate

A limited amount of data was taken using water to depopulate the lower levels. In the supersonic mixing mode, there was not as drastic a change as in the gas-dynamic mode. Figure 34 shows the burn pattern changes due to H_2O for two sets of data. In both graphs, the addition of water lengthens the burn pattern and increases the total intensity over all but the upstream edge of the mirror. In that region the intensity is not appreciably affected.

6.6 Additional Factors Affecting Performance

Several factors have not been considered so far. Certainly the length of time the laser is operated will affect the amount of energy obtained. For the data presented here, run times have been held constant to within ±0.1 second in order to minimize this effect. As mentioned earlier, power readings increase for several seconds of operation and then slightly drop. (This point varies with the gas flow rates and associated temperature.) Therefore, much of the data presented might be different if the hardware remained at a constant temperature.

It was found that varying the electrical input power produces an effect that would be expected. With lower input power, lower

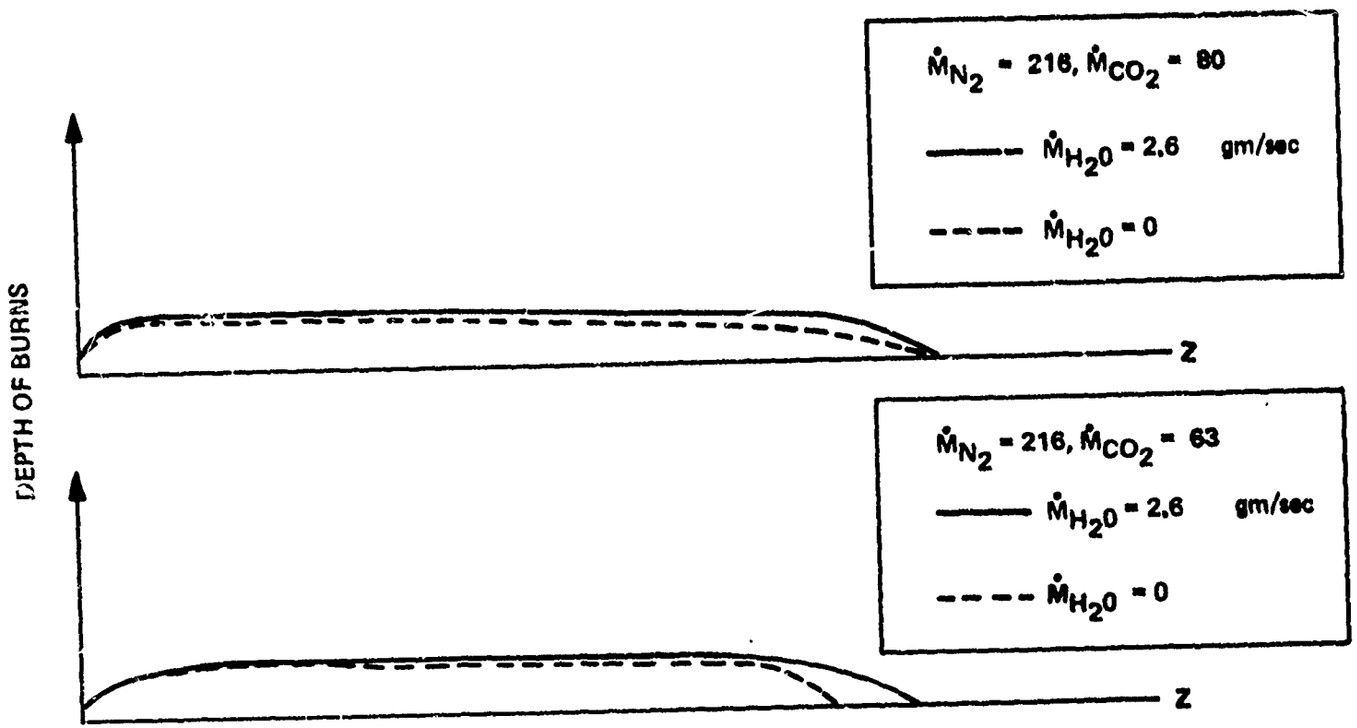

FIGURE 34. SPATIAL BURN PATTERNS WITH H_2O VARIATION (MODE II)

temperatures T_o are obtained. Burn patterns remain about the same in shape, yet reduced in depth, or intensity. Again, this factor was held constant for the data presented.

After operation of the SCL for some time, mirror and window surfaces deteriorate. This problem was minimized by recording data as near in time as possible to other data which would be used for comparison. The data presented has been carefully selected in order to keep all parameters as constant as possible for each illustration or graph. In some instances, it is not possible to easily compare one figure with another. This is especially true concerning output power values. The burn patterns remain about the same in shape but the quantitative power levels change.

6.7 Summary of Mode II Operation

Operation of the SCL utilizing supersonic mixing may be summarized as follows. Not much power variation is observed as the N_2 flow rate is increased, once sufficient flow is obtained. Outputs increase almost linearly with the CO_2 flow, over the range studied. The addition of helium causes the upstream intensity peak to be decreased and the entire beam made smoother. H_2O increases the burn length and raises the intensity slightly.

It is possible that He is not only depopulating the lower states but also depopulating the upper lasing state. This would tend to decrease the inversion peak at the upper end of the cavity. Since the lower levels are depopulated faster than without helium, the inversion exists for a further distance downstream.

Other parameters, such as input power and time of operation, affect the beam as would be expected.

CHAPTER 7

DISCUSSION AND RECOMMENDATIONS

Certain observations and conclusions may be drawn from the data presented here. Perhaps most obvious is the difference in performance of Modes I and II. This chapter compares the two types of operation. In addition, recommendations are given for further work in this field.

7.1 Comparison of Modes I and II

The immediate difference noted between Mode I and Mode II operation is the increase of output power in Mode II. The gas-dynamic operation in Mode I produced a maximum of 15 watts. With the supersonic mixing in Mode II, up to 275 watts were obtained.

This does not imply that supersonic mixing produces a more efficient or powerful CO_2 system than a gas-dynamic one. It must be remembered that the SCL was operated under marginal gas-dynamic conditions. Temperatures and pressures for both modes of operation would ideally have been different.

However, the data furnished here does imply that the range of plenum conditions necessary for lasing action is considerably extended in Mode II. Output power was obtained in Mode I only by the addition of water vapor in a very narrow percentage range: between 2 and 6 percent. No detectable output was obtained while using helium to

depopulate the lower levels. Lasing was obtained in Mode II for nearly all the gas ratios and flow rates that were used.

Maximum output in Mode I was at 3 percent water, 8 to 10 percent CO_2, and with the remainder N_2. P_o and T_o were near 2 atmospheres and 1400°K, respectively. In Mode II, maximum output was with 17 percent CO_2, 83 percent N_2, and no helium or water. P_o was 4 atmospheres and T_o was 1500°K. In both cases the electrical input was near 1 megawatt.

7.2 Recommendations and Plans for Future Work

Several suggestions may be given for further study of gas-dynamic and related systems. Certainly additional work is necessary for optimization of flow mixtures, ratios, and rates. Additional work in nozzle design may prove to be most useful. Methods of coupling energy out of the cavity need to be improved in several respects.

Concerning the SCL facility itself, a number of improvements are to be desired. The hardware needs to be redesigned so that it may reach optimum gas-dynamic conditions. Certain parts need to be cooled in some manner. It is quite likely that a longer cavity (in the direction of flow) might increase performance without the need for changing any of the flow characteristics.

At the present time, several of these and other improvements are being incorporated into the SCL. A two-arc system is being assembled and tested. A larger, water-cooled, and more versatile plenum has been constructed, along with a new nozzle design. This nozzle will allow thermal mixing in the near-sonic region immediately upstream of the throat. (Only a limited amount of study has previously

been done in this Mode III operation.) Methods of mounting and adjusting the cavity mirrors are also being changed.

The new system should be quite useful in investigations which were not completed in the older system. Besides furnishing more efficient and powerful operation, a number of parametric studies may be made in the future, including the effects of controlled amounts of impurities. Mixture ratios may be further optimized. The system may also be adapted to a different lasing scheme. Perhaps most important, information concerning other more sophisticated aerodynamic systems may be deduced from results obtained with the SCL.

REFERENCES

1. Basov, N. G., and Oraevskii, A. N., "Attainment of Negative Temperatures by Heating and Cooling of a System," J. Exptl. Theoret. Phys., 44, USSR, 1963, pp. 1742-5 (Soviet Phys. JETP, 17, 1963, pp. 1171-2).

2. Hurle, I. R., Hertzberg, A., and Buckmaster, J. D., Cornell Aeronautical Laboratory Report RH-1670-A-1, 1962.

3. Hertzberg, A., and Hurle, I. R., "On the Possible Production of Population Inversion by Gas-Dynamic Techniques," Bull. Am. Phys. Soc., 9, 1964, p. 582.

4. Roberts, T. G., Hutcheson, G. J., Ehrlich, J. J., Hales, W. L., and Barr, T. A., "High-Power N_2-CO_2-He Laser Development," IEEE J. of Quan. Elec., QE-3, 1967, pp. 605-9.

5. Horrigan, F. A., Klein, C. A., Rudko, R. I., Wilson, D. T., "High Power Gas Laser Research," Final Technical Report on Contract DA-AH01-67-1589, September 1968.

6. Hurle, I. R., and Hertzberg, A., "Electronic Population Inversion by Fluid-Mechanical Techniques," Phys. Fluids, 8, 1965, pp. 1601-7.

7. Konyukhov, V. K., and Prokhorov, A. M., "Population Inversion in Adiabatic Expansion of a Gas Mixture," ZhETF Pis'ma, 3, USSR, 1966, pp. 436-9 (JETP Letters, 3, 1966, pp. 286-8).

8. Wilson, J., "Nitrogen Laser Action in a Supersonic Flow," Appl. Phys. Lett., 8, 1966, pp. 159-61.

9. Gudzenko, L. I., Filippov, S. S., and Shelepin, L. A., "Rapid Recombination of Plasma Jets," J. Exptl. Theoret. Phys., 51, USSR, 1966, pp. 1115-9 (Soviet Physics JETP, 24, 1967, pp. 745-8).

10. Basov, N. G., Oraevskii, A. N., and Shcheglov, V. A., "Thermal Methods for Laser Excitation," Ah. Tekh. Fiz., 37, 1967, pp. 339-48 (Soviet Phys.-Tech. Phys., 12, 1967, pp. 243-9).

11. Treanor, C. E., Rich, J. W., and Rehm, R. G., "Vibrational Relaxation of Anharmonic Oscillators with Exchange-Dominated Collisions," J. Chem. Phys., 48, 1968, pp. 1798-1807.

12. Wisniewski, E. E., Fein, M. E., Verdeyen, J. T., and Cherrington, B. E., "Thermal Production of a Population Inversion in Carbon Dioxide," Appl. Phys. Lett., 12, 1968, pp. 257-8.

13. Leonard, R. L., Ahlstrom, H. G., and Hertzberg, A., "Stimulated Emission in the MPD Arc," Bull. Am. Phys. Soc., 13, 1968, p. 1591.

14. Fein, M. E., Verdeyen, J. T., and Cherrington, B. E., "A Thermally Pumped CO_2 Laser," Appl. Phys. Lett., 14, 1969, pp. 337-40 and Appl. Phys. Lett., 15, 1969, p. 128.

15. Basov, N. G., Mikhailov, V. G., Oraevskii, A. N., and Shcheglov, V. A., "Molecular Population Inversion in the Supersonic Flow of a Binary Gas in a Laval Nozzle," Ah. Tekh. Fiz, 38, 1968, pp. 2031-41 (Soviet Phys.-Tech. Phys., 13, 1969, pp. 1630-6).

16. Bronfin, B. R., Boedeker, L. R., and Cheyer, J. P., "Thermal Laser Excitation by Gas Dynamic Mixing in Supersonic Flow," Bull. Am. Phys. Soc., 14, 1969, p. 857.

17. Kuehn, D. M., and Monson, D. J., "Experiments with a CO_2 Gas-Dynamic Laser," Appl. Phys. Lett., 16, 1970, pp. 48-50.

18. Biryukov, A. S., Gordiets, B. F., and Shelepin, L. A., "Vibrational Relaxation and Population Inversion in the CO_2 Molecule in Non-stationary Conditions," J. Exptl. Theoret. Phys., 57, USSR, 1969, pp. 585-99 (Soviet Physics JETP, 30, 1970, pp. 321-8).

19. Bronfin, B. R., Boedeker, L. R., and Cheyer, J. P., "Thermal Laser Excitation by Mixing in a Highly Convective Flow," Appl. Phys. Lett., 16, 1970, pp. 214-7.

20. Gerry, E. T., "Gas-Dynamic CO_2 Lasers," Bull. Am. Phys. Soc., 15, 1970, p. 563.

21. News Report, "CO_2 'Rocket' Laser Puts Out 60 KW," Industrial Research, 12, 1970, pp. L3-L4.

22. News Report, Laser Focus, 6, 1970, pp. 16, 18.

23. Taylor, R. L., and Bitterman, S., "Vibrational Energy Transfer in the CO_2-N_2 Molecular System," Bull. Am. Phys. Soc., 13, 1970, p. 1591.

24. Glick, H. S., Squire, W., and Hertzberg, A., "A New Shock Tube Technique for the Study of High Temperature Gas Phase Reactions," Fifth Symposium (International) on Combustion, 1955, pp. 393-402.

25. Stollery, J. L., and Smith, J. E., "A Note on the Variation of Vibrational Temperature Along a Nozzle," J. Fluid Mech., 13, 1962, pp. 225-36.

26. Patel, C. K. N., Faust, W. L., and McFarlane, R. A., "CW Laser Action on Rotational Transitions of the $\Sigma_u^+-\Sigma_g^+$ Vibrational Band of CO_2," Bull. Am. Phys. Soc., 9, 1964, p. 500.

27. Patel, C. K. N., "Continuous-Wave Laser Action on Vibrational-Rotational Transitions of CO_2," Phys. Review, 136, 1964, pp. A1187-93.

28. Patel, C. K. N., "Selective Excitation Through Vibrational Energy Transfer and Optical Maser Action in N_2-CO_2," Phys. Review Lett., 13, 1964, pp. 617-9.

29. Patel, C. K. N., "CW High Power N_2-CO_2 Laser," Appl. Phys. Lett., 7, 1965, pp. 15-7.

30. Howe, J. A., "Effect of Foreign Gases on the CO_2 Laser: R-Branch Transitions," Appl. Phys. Lett., 7, 1965, pp. 21-2.

31. Witteman, W. J., "Increasing Continuous Laser-Action on CO_2 Rotational Vibrational Transitions Through Selective Depopulation of the Lower Laser Level by Means of Water Vapor," Phys. Lett., 18, 1965, pp. 125-7.

32. Moeller, G., and Rigden, J. D., "High-Power Laser Action in CO_2-He Mixtures," Appl. Phys. Lett., 7, 1965, pp. 274-6.

33. Rosenberger, D., "The Influence of Hydrogen on the Output of a N_2-CO_2 Laser," Phys. Lett., 21, 1966, pp. 520-1.

34. Witteman, W. J., "Inversion Mechanisms, Population Densities and Coupling-Out of a High-Power Molecular Laser," Philips Research Reports, 21, 1966, pp. 73-84.

35. Barr, T. A., "The Army Missile Command 8,000 KW Plasma Facility," Fourth Space Congress, Canaveral Council of Technical Societies, Session 25, 1967, pp. 1-9.

36. Barr, T. A., and Cason, C., "Multiple Arc Performance in an 8000 KW Plasma Facility," Eighth Symposium on Engineering Aspects of Magnetohydrodynamics, 1967, pp. 145-47.

37. Barr, T. A., and Mayo, R. F., "A 'Spark-Plug' Starter for Arc Plasma Generators," J. Spacecraft Rockets, 2, 1965, pp. 808-10.

38. Van Wylen, G. J., Thermodynamics, 1959, pp. 343-99.

39. Weast, R. C. (Editor-in-Chief), Handbook of Chemistry and Physics, 45th Edition, 1964, pp. E-47-E-55.